Biogeosciences, 9, 973–992, 2012
www.biogeosciences.net/9/973/2012/
doi:10.5194/bg-9-973-2012

Biogeosciences

Insignificant enhancement of export flux in the highly productive subtropical front, east of New Zealand: a high resolution study of particle export fluxes based on ^{234}Th: ^{238}U disequilibria

K. Zhou[1], **S. D. Nodder**[2], **M. Dai**[1], **and J. A. Hall**[2]

[1]State Key Lab of Marine Environmental Science, Xiamen University, Xiamen, China
[2]National Institute of Water and Atmospheric Research Ltd. (NIWA), Private Bag 14-901, Wellington, New Zealand

Correspondence to: M. Dai (mdai@xmu.edu.cn)

Received: 10 September 2011 – Published in Biogeosciences Discuss.: 21 September 2011
Revised: 17 January 2012 – Accepted: 23 January 2012 – Published: 12 March 2012

Abstract. We evaluated the export fluxes of Particulate Organic Carbon (POC) in the Subtropical Frontal zone (STF) of the SW Pacific sector of the Southern Ocean. The site is characterized by enhanced primary productivity, which has been suggested to be stimulated through so-called natural iron fertilization processes where iron-depleted subantarctic water (SAW) mixes with mesotrophic, iron-replete subtropical water (STW). We adopted the small-volume ^{234}Th method to achieve the highest possible spatial sampling resolution in austral late autumn-early winter, May-June, 2008. Inventories of chlorophyll-*a*, particulate ^{234}Th and POC observed in the upper 100 m were all elevated in the mid-salinity water type ($34.5 < S < 34.8$), compared with low salinity waters ($S < 34.5$) which were of SAW origin with high macronutrients and high ($S > 34.8$) salinity waters which were of STW origin with low macronutrients. However, Steady-State ^{234}Th fluxes were similar across the salinity gradient being, 25 ± 0.78 ($(1.5 \pm 0.047) \times 10^3$) in the mid-salinity, and 29 ± 0.53 ($(1.8 \pm 0.032) \times 10^3$) and 22 ± 1.1 Bq m^{-2} d^{-1} ($(1.3 \pm 0.066) \times 10^3$ dpm m^{-2} d^{-1}) in the high and low salinity waters respectively. Bottle POC/Th ratios at the depth of 100 m were used to convert ^{234}Th fluxes into POC export fluxes. The derived POC flux did not appear to be enhanced in mid-salinity waters where the primary productivity was inferred to be the highest at the time of sampling, with a flux of 11 ± 0.45 mmol C m^{-2} d^{-1}, compared to 14 ± 0.39 mmol C m^{-2} d^{-1} in high salinity waters and 8.5 ± 0.66 mmol C m^{-2} d^{-1} in low salinity waters. This study thus implied that natural iron fertilization does not necessarily lead to an enhancement of POC export in STF regions.

1 Introduction

The Subtropical Front (STF) (Fig. 1a) is a circum-global oceanographic feature, typically between about 35° S and 45° S, where cold, high macro-nutrient, iron-limited subantarctic waters (SAW) mix with warm, low macro-nutrient, subtropical waters (STW) (Longhurst, 1998; Orsi et al., 1995). A number of studies have shown enhanced year-round chlorophyll concentrations and primary production (PP) in the STF region (Behrenfeld and Falkowski, 1997; Comiso et al., 1993; Murphy et al., 2001). The observed PP in the STF, east of New Zealand, can be as high as 22 mmol C m^{-2} d^{-1} in winter, which may be more than 4 and 2-times higher than in the adjacent SAW and STW, respectively (Bradford-Grieve et al., 1997). Similarly elevated integrated production rates have been observed in the STF around 152° E off Australia in summer (Clementson et al., 1998) and in the South African sector at 20° E in winter (Froneman et al., 1999). Such enhancement in PP in the STF zone has been suggested to be induced by natural iron fertilization processes, with the iron sourced from atmospheric deposition, shelf boundary exchange processes and/or mixing with iron-replete subtropical waters (Boyd et al., 1999, 2004; Pollard et al., 2009).

To the east of New Zealand, the STF is constrained bathymetrically along a prominent submarine ridge, the Chatham Rise (Heath, 1985; Uddstrom and Oien, 1999; Sutton, 2001). Like other STF zones, this site is the transition zone from mesotrophic STW in the North, characterized by the relatively high temperatures (summer >18 °C; winter >14 °C), salinities (>35.1) and dissolved

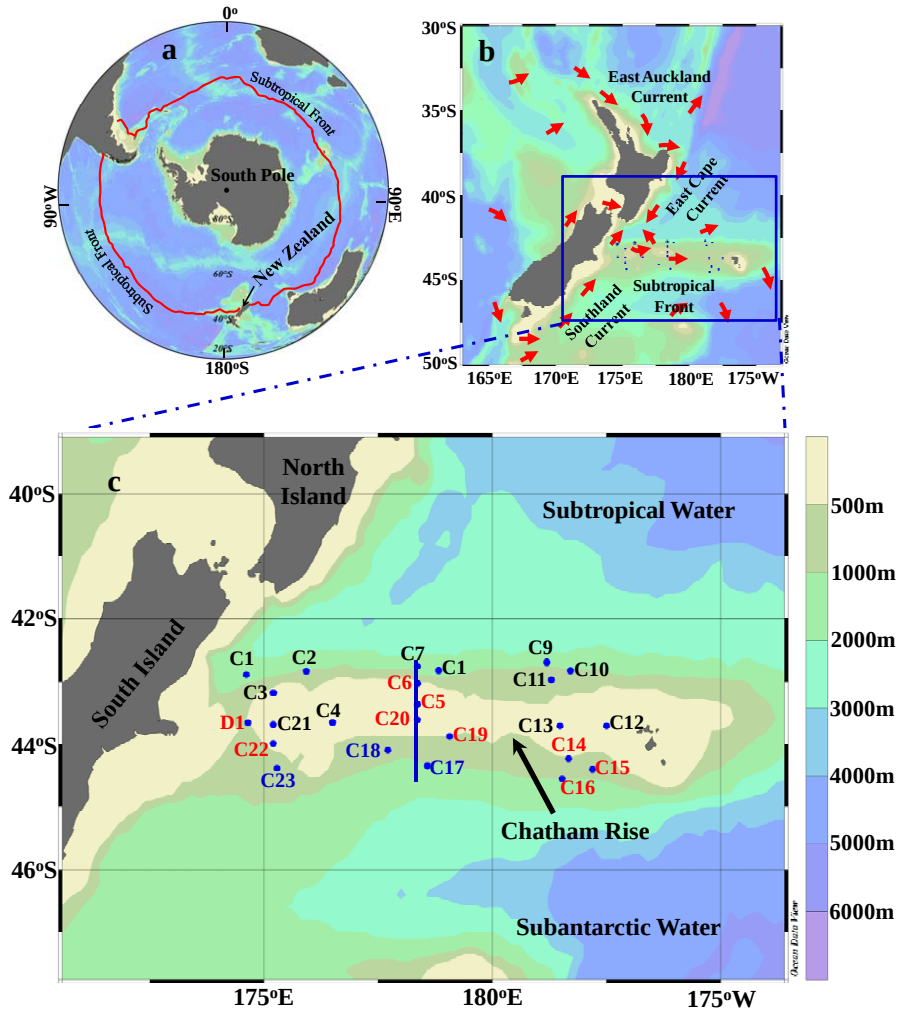

Fig. 1. Hemispherical map of the Southern Ocean showing the approximate location of the Subtropical Front as a red line **(a)**, with the map of the study area showing the mean circulation and surface water masses (Nodder, 1997) **(b)**; the location of sampling sites during the May-June 2008 research cruise TAN0806 **(c)**; and the stations with salinities >34.8 (high), 34.5–34.8 (mid), and <34.5 (low) marked in black, red, and blue, respectively. The blue line represents the transect where stations were sampled throughout the water column (Transect M). The bathymetry of the study area is also shown to emphasize the location of the Chatham Rise.

iron levels (>0.2 nmol l^{-1}), and low macronutrient concentrations (e.g. PO_4 <0.3 µmol l^{-1}), to high nutrient-low chlorophyll (HNLC) SAW to the south, with typically low temperatures (summer <14 °C; winter <10 °C), low salinities (<34.6) and low iron levels (<0.1 nmol l^{-1}), but high macronutrient concentrations (e.g. PO_4 >0.9 µmol l^{-1}) (Boyd et al., 1999; Nodder, 1997). Regardless of seasonal and spatial variations, phytoplankton biomass and biological productivity are generally elevated over the Chatham Rise (Bradford-Grieve et al., 1997, 1999; Gall et al., 1999). In winter and spring, average chlorophyll *a* (Chl-*a*) concentrations, integrated down to 100 m, can reach up to ~80 mg m^{-2}, and the corresponding PP, integrated to 1 % light level, can be more than 50 mmol C m^{-2} d^{-1} (Bradford-Grieve et al., 1997). In comparison, the average inventory of Chl-*a* and PP may be only 13 mg m^{-2} and 12 mmol C m^{-2} d^{-1}, respectively, in SAW and 33 mg m^{-2} and 46 mmol C m^{-2} d^{-1} in STW. Such perennially high PP levels in the STF support a diverse planktonic and benthic ecosystem (Probert and McKnight, 1993; Bradford-Grieve et al., 1999) that seems to be translated to many fish species, with New Zealand's richest deep-water fisheries, primarily in blue grenadier (known locally as hoki, *Macruronus novaezelandiae*) and orange roughy (*Hoplostethus atlanticus*), occurring on the Chatham Rise (New Zealand Ministry of Fisheries, 2009).

However, little is known thus far about the spatio-temporal variability and magnitude of the downward export of particulate organic carbon (POC), or the fate of the PP in this frontal zone. Nodder (1997) used free-floating cylindrical sediment

traps in the vicinity of the STF showing that the POC flux was less than 3 mmol C m^{-2} d^{-1}, which is in the same order of magnitude as that found in low export oligotrophic oceans. Indirect evidence from benthic studies, however, indicates that organic fluxes are enhanced on the crest and southern flank of the Chatham Rise (Probert and McKnight, 1993; Nodder et al., 2003). It is thus clear that information on the spatial variation of POC export within the STF is required if we are to evaluate whether the enhanced primary production in the frontal zone also leads to enhanced export production.

In the present study, we utilized a particle-reactive radionuclide, ^{234}Th ($t_{1/2} = 24.1$ d), as a tracer for particle export from the upper ocean. The technique has been applied widely in many oceanographic settings to examine processes occurring on time-scales of days to weeks (e.g. Coale and Bruland, 1985, 1987; Buesseler, 1992, 1998; Cochran and Masque, 2003; Dai and Benitez-Nelson, 2001; Waples et al., 2006). A further technological advantage is the use of the recently developed small-volume technique that enables high resolution sampling (Benitez-Nelson et al., 2001a; Buesseler et al., 2001a; Cai et al., 2006a). This method is essential in order to capture the particle dynamics and export flux variability in such regions as the STF, which are characterized by dynamic hydrography (e.g., Cai et al. 2008; Buesseler et al., 2009). Indeed, with high resolution sampling, Cai et al. (2008) observed significant variations of ^{234}Th deficit in the South China Sea, with enhanced Th and POC fluxes along the western and southern boundaries of this marginal sea. Buesseler et al. (2009) even observed high spatial variability in the northern subtropical gyre at ALOHA station off Hawaii, where a homogenous spatial distribution of POC flux from the surface ocean would have been expected.

The present study aims to examine the spatial distribution, magnitude and variability of upper ocean POC export in the STF over the Chatham Rise to the east of New Zealand by using high spatial resolution sampling of ^{234}Th. We show that ^{234}Th-based POC export is not significantly enhanced in the frontal zone, despite high Chl-*a* and inferred PP levels, compared to the adjacent SAW and STW.

2 Methods

2.1 Sample collection

Samples were collected in late austral autumn-early winter from 23 May to 12 June in 2008 on board R/V Tangaroa, operated by the National Institute of Water and Atmospheric Research (NIWA) Ltd, New Zealand (NIWA voyage TAN0806). High spatial resolution sampling at 23 stations, covering a surface area of about 25 000 km^2, was conducted during the cruise (Fig. 1). Water samples were collected using 10 l Niskin bottles mounted on a rosette sampler attached to a Seabird SBE9/11plus conductivity-temperature-depth (CTD) sensor. A sub-sample of 4 l seawater was used to determine the total ^{234}Th activity (see below) and another 8 l was filtered onto a 25-mm diameter Quartz Microfiber (QMA, norminal pore size ~1.0 µm) for particulate ^{234}Th and POC measurements. Samples were collected at 5 depths in the upper 100 m (normally 10, 20, 50, 70, and 100 m), except along transect M where sampling was conducted at a finer depth resolution throughout the water column to better define the vertical structure of ^{234}Th over the Chatham Rise (shown as a blue line in Fig. 1). Since this was the first ^{234}Th study over the Chatham Rise, such an intensive sampling strategy enabled a robust description of both the vertical and spatial distribution of ^{234}Th.

2.2 ^{234}Th analysis

We used the small-volume MnO_2 co-precipitation technique for our total ^{234}Th analyses, as initially developed by Benitez-Nelson et al. (2001a) and Buesseler et al. (2001a), and further modified by Cai et al. (2006a). Four litre seawater samples were immediately acidified with 6 ml concentrated HNO_3 and spiked with ~166.7 mBq ^{230}Th after collection. The samples were then mixed vigorously and allowed to stand for 12 h for isotopic equilibration. The pH was then brought up to 8.00–8.20 and thorium isotopes were co-precipitated with MnO_2 by adding 0.25 ml $KMnO_4$ (3.0 g l^{-1}) and 0.25 ml $MnCl_2$ (8.0 g $MnCl_2 \cdot 4H_2O$ l^{-1}). The formation of the MnO_2 precipitate was accelerated by heating to approximately 90 °C in a water bath for 2 h. The precipitate was then filtered onto a 25 mm QMA filter after samples were cooled to room temperature. The QMA filter was baked at about 100–200 °C until dryness, and then mounted under a layer of Mylar and two layers of aluminum foil (total density ~7.2 mg m^{-2}) for beta-counting at sea by a gas-flow proportional low-level RISØ beta-counter (Model GM-25-5, RISØ National Laboratory, Denmark). These samples were re-counted for background levels 6 months after the cruise (i.e., >5 half-lives of ^{234}Th).

The QMA filter used for particulate ^{234}Th determination was dried at 50 °C in an oven for 24 h, and then mounted and beta-counted as above for the total ^{234}Th. The average background levels for total and particulate ^{234}Th were 0.45 and 0.32 counts per minute (cpm), respectively.

We used an alpha spectrometric method for our total ^{234}Th recovery analysis (Cai et al., 2006a). Samples were demounted after background counting, spiked with ~166.7 mBq ^{228}Th (^{232}U-^{228}Th solution) and then digested by adding 10 ml concentrated HNO_3, 1 ml HF and 1 ml H_2O_2. Thorium isotopes were purified through iron precipitation and a classic anion column. Eluents were then evaporated onto a 25 mm stainless steel disc after extraction using 1.5 ml of 0.25 mol l^{-1} theonyl trifluoroacetone(TTA)/benzene solution. The disc was counted by alpha spectrometry (Octete ^{TM} PC) until both thorium isotopes (^{230}Th and ^{228}Th) reached more than 2,500 counts. Most of

the final recoveries for ^{230}Th were between 80 % and 103 %. The average of the recoveries was 90.2 ± 1.4 % (mean $\pm$ 1 standard deviation). The errors associated with ^{234}Th activity determination are propagated from the counting errors on the first counts, background measurements and recovery analyses. The precision of the final ^{234}Th activity was better than 5 %.

Instead of undertaking specific sample analyses, we used the relationship: A_U (mBq l^{-1}) = 1.1801 $\times$ salinity to estimate the ^{238}U activity (A_U) in the seawater according to Chen et al. (1986). The uncertainty of ^{238}U activity was $\sim$3 % which was also included in the error estimates associated with the ^{234}Th fluxes.

2.3 POC and Particulate Nitrogen (PN) analysis

After beta-counting for particulate ^{234}Th, the samples were demounted for POC and PN analysis. The filters were placed in Petri dishes and fumed using concentrated hydrochloric acid for 24 h to remove the carbonate phase. POC concentrations were then determined by a PE-2400 SERIES II CHNS/O analyzer, according to JGOFS protocols (Knap et al., 1996). Replicate procedural C blanks from sampling to instrumental carbon determination have been tested before (Chen, 2008), and were all less than 6 µg C and 2 µg N, which typically accounted for less than 10 % of the sample POC and PN, respectively. The precision for our POC measurements were always better than 10 % (Cai et al., 2006a; Chen, 2008).

2.4 Other ancillary parameters

The temperature and salinity vertical profile data were obtained from the Seabird SBE9/11plus CTD. A Wetlabs fluorometer, interfaced with the CTD, was used to determine the fluorescence at an excitation and emission wavelength of 470 and 695 nm. In order to calibrate the fluorometer, discrete seawater samples (1–2 l) were collected for the measurement of Chl-*a*. Briefly, seawater was filtered through a Whatman GF/F filter, and Chl-*a* on the filter was then extracted with 90 % acetone and analyzed using a spectrofluorometer. A linear relationship was found between fluorescence and Chl-*a* (Chl-*a* (µg l^{-1}) = 0.639 $\times$ Fluorescence, $R^2 = 0.87$, $n = 50$), which was then applied to convert the fluorescence values into Chl-*a* concentrations. Uncertainties for the Chl-*a* determination were <10 %.

Macronutrients were determined using classic colorimetric method (Ellwood and Maher, 2003). The detection limits for dissolved inorganic nitrogen (DIN, nitrate plus nitrite), PO_4 and $Si(OH)_4$ were 0.07 µmol l^{-1}, 0.03 µmol l^{-1} and 0.07 µmol l^{-1}, respectively.

3 Results

3.1 Hydrography

The complex hydrological characteristics of the STF are shown by the relationship between potential temperature and salinity in Fig. 2. In the upper ocean, distinctly different water characteristics were found between stations, representing different degrees of mixing. The surface temperature and salinity changed dramatically over the sampled area from lows of 9.4 °C and 34.2, respectively, in surface waters with SAW affinities, to highs of 15.2 °C and 35.2 in surface waters associated with STW.

Figure 3 shows the spatial distributions of temperature and salinity at 2 m and 100 m water depths. The gradients of salinity and temperature were much greater in the region between 43° S and 44° S, coinciding with the crest and upper southern flank of the Chatham Rise. Vertically, the surface 150 m of all stations sampled in the STF was well stratified (Fig. 4a, b, and c). However, the depth of the surface isothermal mixed-layer, defined by the density surface with a 0.5 °C temperature difference from the reference depth (Kara et al., 2000), was not uniform between stations, ranging from 54 m to 178 m. Typically and as illustrated in Fig. 4, the depth of the mixed-layer at high salinity stations was deeper than at mid- and low salinity stations (see next section for definitions of water types).

3.2 Chl-*a*, macronutrient, and POC distribution

Vertically, Chl-*a* was highest within the upper mixed-layer. Below the mixed-layer, the Chl-*a* concentration decreased to background, effectively zero (Fig. 4a, b). Regionally, Chl-*a* concentrations were elevated where salinities were between 34.5 and 34.8 (Fig. 2b). In such cases, the average Chl-*a* concentration in the upper 100 m was as high as 0.79 µg l^{-1} compared to 0.40 µg l^{-1} at salinities >34.8 or 0.37 µg l^{-1} at salinities <34.5. Accordingly, for the ease of discussion, we have divided the STF waters of our study area into three different water types: low ($S < 34.8$), mid- ($34.5 < S < 34.8$) and high salinity ($S > 34.8$), according to the vertical and horizontal distribution of Chl-*a*.

Both DIN and PO_4 concentrations were generally at replete levels during the cruise. In the upper 100 m, DIN concentrations ranged from 3.6 µmol l^{-1} to 13.9 µmol l^{-1} in mid-salinity waters, with an average of 8.9 µmol l^{-1}. In high salinity waters, it was lowest, ranging from 1.1 µmol l^{-1} to 12.3 µmol l^{-1}, with an average of 4.7 µmol l^{-1}. In low salinity waters, DIN concentration varied from 7.8 µmol l^{-1} to 14.9 µmol l^{-1}, with an average of 11.3 µmol l^{-1}, which was the highest among the three water types. PO_4 shared the similar distribution pattern with that of DIN. In mid salinity waters, the average of PO_4 concentration in the upper 100 m was 0.71 µmol l^{-1}, compared to 0.42 µmol l^{-1}in high salinity waters and 0.87 µmol l^{-1} in low salinity waters.

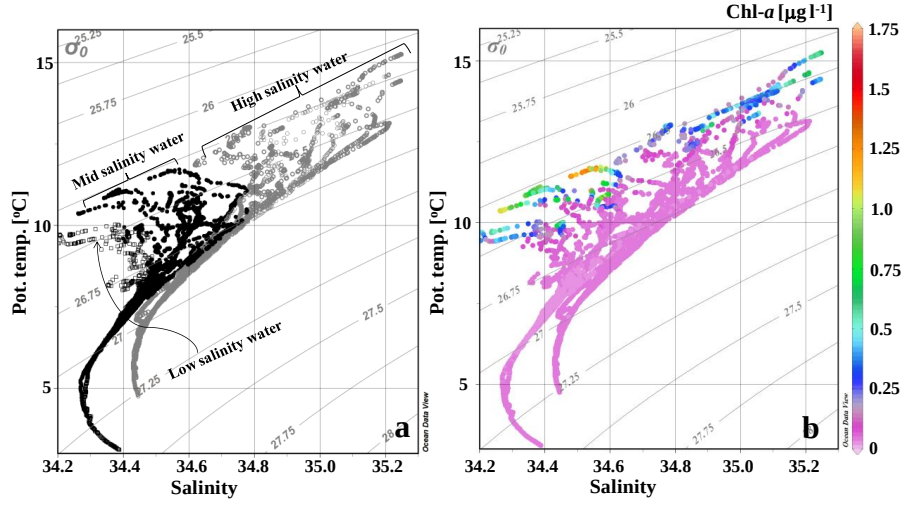

Fig. 2. (a) T-S diagram over the Chatham Rise, east of New Zealand (○ high salinity (S > 34.8) water; ● mid-salinity (34.5 < S < 34.8) water; □ low salinity (S < 34.5) waters). The isopycnal lines are also shown; **(b)** Regional distribution of Chl-*a* plotted on the T-S diagram.

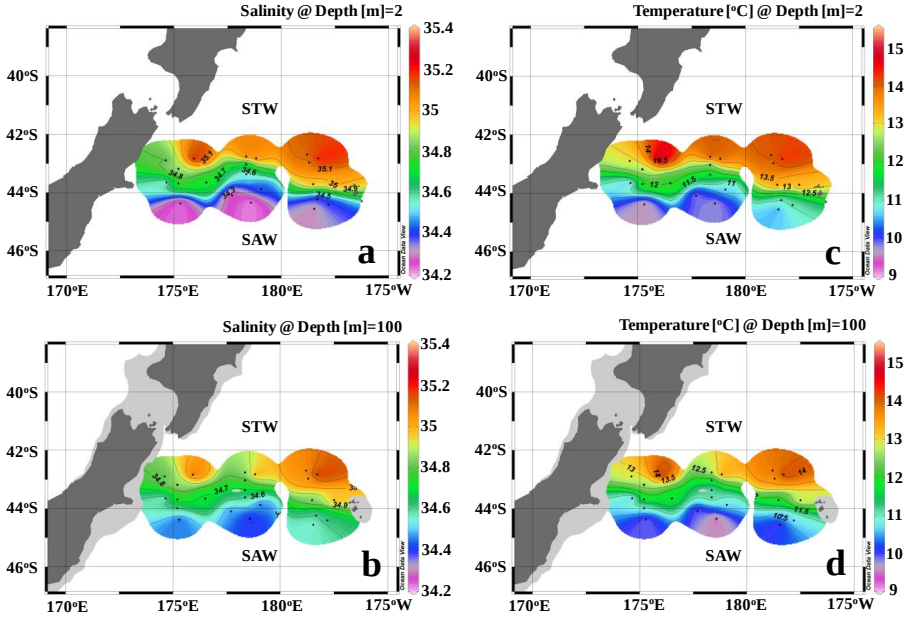

Fig. 3. Distributions of temperature and salinity, highlighting dramatic changes within the Subtropical Frontal zone: **(a)** surface salinity at 2 m water depth, **(b)** salinity at 100 m, **(c)** surface temperature, and **(d)** temperature at 100 m. The Subtropical water (STW) and Subantarctic water (SAW) are also highlighted.

$Si(OH)_4$ was only measured at stations C1 through C7 covering high and mid-salinity waters. Based on the limited $Si(OH)_4$ data set, its concentration in the upper 100 m varied from 0.39 to 3.43 µmol l^{-1} in mid-salinity stations (C5 and C6), which is comparable to the range in the high salinity stations (C1, C2, C3, C4 and C7, 0.91–3.11 µmol l^{-1}). Inventories of these macronutrients are listed in Table 2.

POC concentrations varied from 0.40 µmol C l^{-1} to 6.1 µmol C l^{-1} across the study area (Table 1). In the upper mixed-layer, POC distributions generally followed that of Chl-*a*, indicating a relationship between POC and phytoplankton biomass. Regionally, POC concentration was also relatively enhanced in mid-salinity waters. The average POC concentration in the upper 100 m was 3.9 µmol C l^{-1} in this water type, compared to 2.4 µmol C l^{-1} and 2.6 µmol C l^{-1} in high and low salinity waters, respectively. In a departure

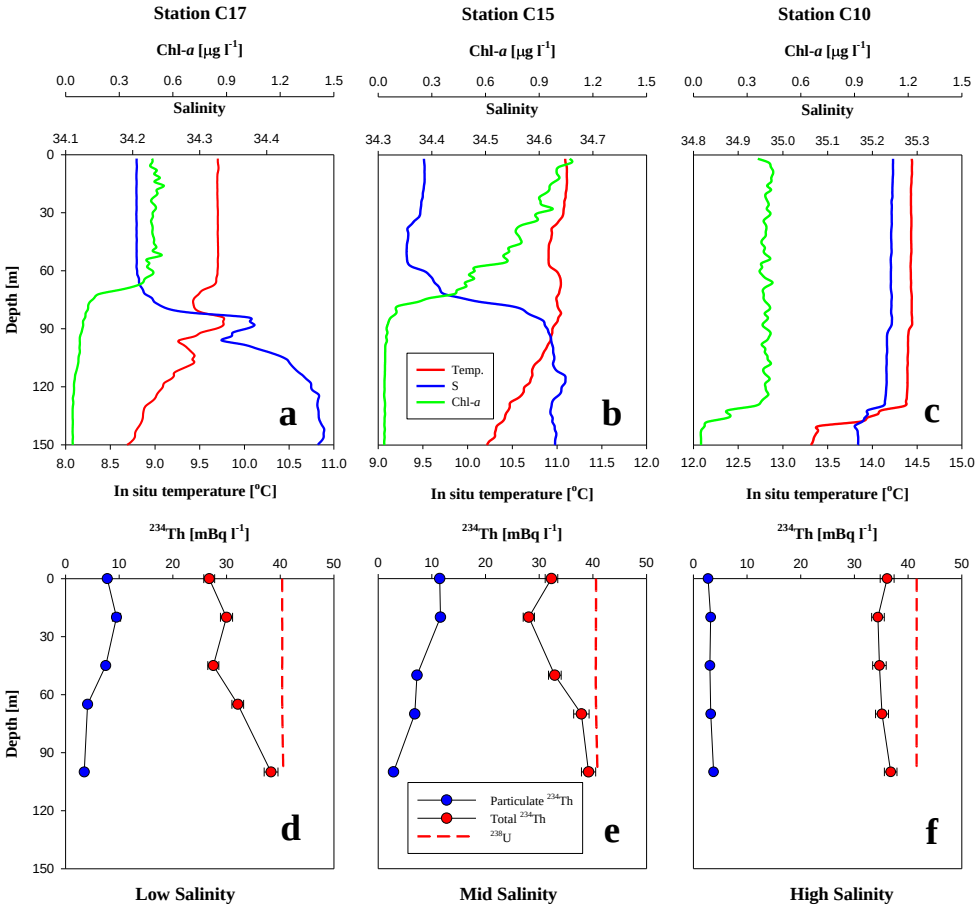

Fig. 4. **(a)**, **(b)**, and **(c)** Vertical profiles of temperature, salinity and Chl-*a* in the upper 100 m at stations C17, C15, and C10, respectively. **(c)**, **(d)**, and **(e)** Vertical profiles of particulate and total ^{234}Th from the same stations.

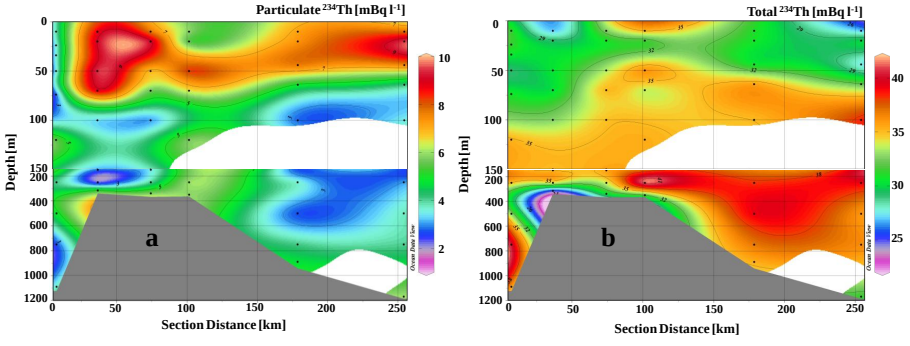

Fig. 5. Sectional distributions of ^{234}Th activity along a meridional transect (Transect M) across the Chatham Rise (see Fig. 1 for transect location): **(a)** particulate ^{234}Th and **(b)** total ^{234}Th.

from the vertical distribution of Chl-*a*, POC concentrations were often higher near the bottom of the water column, which may be indicative of near-bottom sediment resuspension (e.g., Nodder, 1997; Nodder et al., 2007).

The C/N ratio was quite stable in the upper ocean, ranging from 5.2 to 8.5, with an average of 6.6 ± 1.5 ($n = 146$) (mean $\pm$ 1 standard deviation), which is almost identical to the Redfield ratio of 6.63 (Redfield et al., 1963). No obvious changes in C/N ratio were found in association with changes in salinity, suggesting that the particles in the study area were predominantly biogenic in origin.

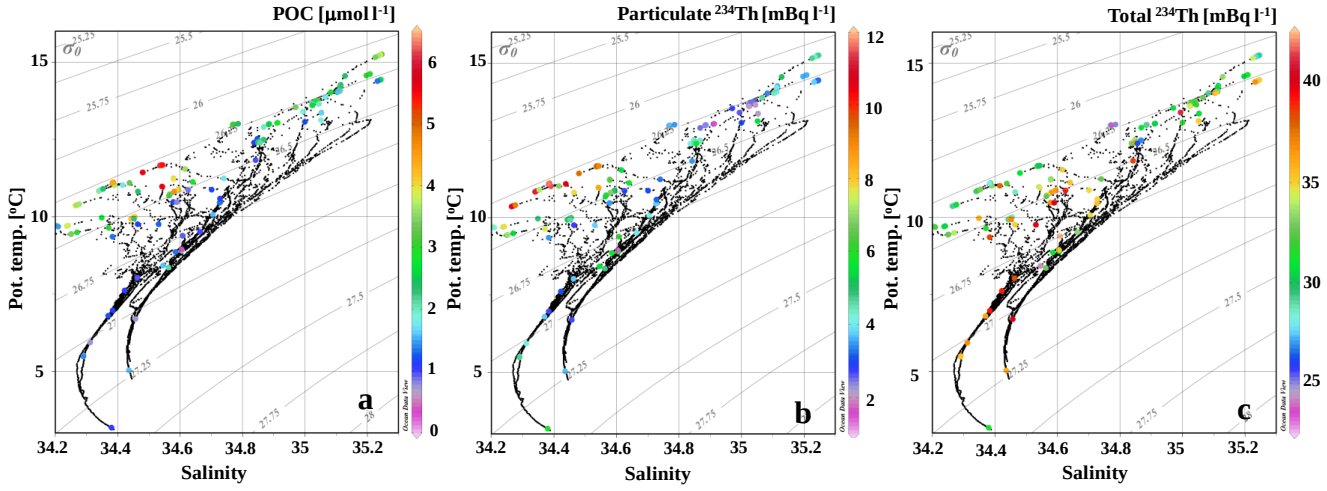

Fig. 6. Regional distributions of: **(a)** particulate organic carbon, **(b)** particulate ^{234}Th, and **(c)** total ^{234}Th plotted on a T-S diagram.

3.3 ^{234}Th distribution

3.3.1 Vertical profiles of ^{234}Th

Particulate and total ^{234}Th activities are listed in Table 1. Profiles of three representative stations from low, mid- and high salinity waters are shown in Fig. 4. The activities of total ^{234}Th varied from 24 ± 1.0 mBq l^{-1} to 42 ± 2.4 mBq l^{-1}. Particulate ^{234}Th activities on suspended particles were variable, ranging from 1.7 ± 0.15 mBq l^{-1} to 12 ± 0.29 mBq l^{-1}. The ^{234}Th activity profile in the upper 100 m was related to the vertical distribution of Chl-*a*. As illustrated in Fig. 4, total ^{234}Th activity was lowest within the isothermal mixed layer. Below the mixed-layer, the activity of total ^{234}Th began to increase as the Chl-*a* leveled off, until it reached secular equilibrium with ^{238}U at the base of the euphotic zone (Ez) where Chl-*a* reached its minimum. At stations with depths of Ez greater than 100 m, the total ^{234}Th activity was in deficit with respect to ^{238}U from 0–100 m. The vertical distribution of particulate ^{234}Th also generally resembled that of Chl-*a* and POC, in that its activity was homogenous within and decreased below the mixed-layer. Not surprisingly, higher particulate ^{234}Th activities were related to higher levels of Chl-*a*, indicating intensive scavenging of biogenic particles in high Chl-*a* waters. However, total ^{234}Th activities seemed to be independent of Chl-*a* and/or biomass. As shown in Fig. 4, for example, the Chl-*a* concentration at the mid-salinity station C15 was twice at the low salinity station C17, but the activities of total ^{234}Th were similar at each station.

3.3.2 Meridional distribution of ^{234}Th

To better describe the spatial distribution pattern of ^{234}Th in the STF across the Chatham Rise, transect M, consisting of stations C5, C6, C7, C17, C18, and C20, was sampled throughout the water column (shown in Fig. 5). Generally, total ^{234}Th was in deficit in upper and near-bottom waters, and was in equilibrium with ^{238}U over the mid-water column. No meridional trends were found in the upper water column along transect M. Particulate ^{234}Th was higher within the Ez and in bottom waters than in the mid-water column. Interestingly, at mid-depths of 300–600 m, a deficit of total ^{234}Th was found in waters on both sides of the Chatham Rise crest. This observation may reflect the horizontal transport of the re-suspended particles along the Chatham Rise flanks, consistent with the near-bottom increases in particle fluxes from sediment trap (Nodder, 1997; Nodder and Northcote, 2001) and benthic studies (Nodder et al., 2007) in the area.

3.3.3 Regional distribution of ^{234}Th

To provide a composite view of the regional distribution of ^{234}Th in relation to different water types, the total and particulate ^{234}Th activities are superimposed on a T/S diagram (Fig. 6). Similar to Chl-*a* and POC, the activities of particulate ^{234}Th in the upper ocean were enhanced in mid-salinity waters, where the average of particulate ^{234}Th activities increased up to 7.5 ± 0.063 mBq l^{-1}, which was two times higher than in the high salinity waters (3.3 ± 0.035 mBq l^{-1}). Noticeably, however, high activities of particulate ^{234}Th were not necessarily correlated with low total ^{234}Th activities. Such a distribution pattern also held for total ^{234}Th among the three water types. The activities of total ^{234}Th in mid-salinity waters varied from 24 ± 3.0 mBq l^{-1} to 42 ± 2.4 mBq l^{-1}, with an average of 33 ± 0.23 mBq l^{-1}, and similarly from 23 ± 0.94 mBq l^{-1} to 41 ± 1.3 mBq l^{-1} in the high salinity waters, with an average of 32 ± 0.16 mBq l^{-1}. In comparison, total ^{234}Th activity ranged from 27 ± 1.0 to 39 ± 1.3 mBq l^{-1} in low salinity waters, with an average of 34 ± 0.32 mBq l^{-1}.

Table 1. Temperature, Salinity, Particulate and Total ^{234}Th activities, ^{238}U activities, ^{234}Th:^{238}U and POC: ^{234}Th ratios for all stations in the Subtropical Front, Chatham Rise, New Zealand, measured in May–June 2008 (NIWA cruise TAN0806).

Depth m	Temp. °C	Salinity	Particulate ^{234}Th mBq l^{-1}	Total ^{234}Th mBq l^{-1}	^{238}U mBq l^{-1}	POC µmol C l^{-1}	^{234}Th:^{238}U	C:Th Ratio mmol C Bq^{-1}
High Salinity Stations								
C1, 174°36′ E, 42°53′ S, 1010 m, 05-24-2008								
10	12.979	34.769	2.8 ± 0.18	24 ± 1.5	41 ± 1.2	2.9 ± 0.29	0.58 ± 0.041	1.0 ± 0.12
20	12.980	34.769	2.4 ± 0.20	28 ± 1.1	41 ± 1.2	2.9 ± 0.29	0.69 ± 0.033	1.2 ± 0.16
50	12.989	34.771	2.5 ± 0.17	29 ± 1.1	41 ± 1.2	2.7 ± 0.27	0.70 ± 0.034	1.1 ± 0.13
70	12.992	34.772	3.7 ± 0.18	23 ± 0.94	41 ± 1.2	3.1 ± 0.31	0.57 ± 0.029	0.86 ± 0.10
100	13.020	34.786	3.4 ± 0.21	25 ± 0.99	41 ± 1.2	2.4 ± 0.24	0.61 ± 0.030	0.70 ± 0.081
C2, 175°56′ E, 42°50′ S, 687 m, 05-25-2008								
10	15.256	35.247	4.7 ± 0.21	27 ± 1.4	42 ± 1.3	3.3 ± 0.33	0.66 ± 0.040	0.70 ± 0.077
20	15.234	35.242	4.8 ± 0.23	31 ± 1.1	42 ± 1.3	3.8 ± 0.38	0.74 ± 0.034	0.80 ± 0.089
50	15.207	35.235	4.3 ± 0.20	27 ± 1.1	42 ± 1.3	3.7 ± 0.37	0.66 ± 0.033	0.86 ± 0.095
70	15.168	35.226	4.7 ± 0.21	34 ± 1.6	42 ± 1.3	3.4 ± 0.34	0.82 ± 0.045	0.73 ± 0.080
100	14.564	35.129	5.1 ± 0.23	31 ± 1.1	42 ± 1.2	2.4 ± 0.24	0.76 ± 0.035	0.46 ± 0.051
C3, 175°13′ E, 43°11′ S, 125 m, 05-26-2008								
10	12.983	34.885	2.5 ± 0.19	27 ± 1.3	41 ± 1.2	2.8 ± 0.28	0.66 ± 0.036	1.1 ± 0.14
20	12.990	34.884	2.6 ± 0.20	32 ± 1.1	41 ± 1.2	2.8 ± 0.28	0.78 ± 0.036	1.1 ± 0.14
50	13.002	34.886	2.5 ± 0.18	24 ± 1.1	41 ± 1.2	2.8 ± 0.28	0.59 ± 0.031	1.2 ± 0.14
70	12.998	34.884	2.4 ± 0.17	29 ± 1.0	41 ± 1.2	2.5 ± 0.25	0.71 ± 0.033	1.1 ± 0.13
100	12.917	34.868	2.4 ± 0.20	31 ± 1.1	41 ± 1.2	2.0 ± 0.20	0.75 ± 0.034	0.82 ± 0.11
C3-2[a], 06-11-2008								
10	12.487	34.867	4.2 ± 0.62	27 ± 1.8	41 ± 1.2	2.4 ± 0.24	0.66 ± 0.049	0.56 ± 0.10
20	12.490	34.867	3.3 ± 0.68	25 ± 2.3	41 ± 1.2	2.0 ± 0.20	0.61 ± 0.059	0.61 ± 0.14
50	12.490	34.867	4.2 ± 0.60	25 ± 1.8	41 ± 1.2	2.1 ± 0.21	0.61 ± 0.047	0.48 ± 0.084
70	12.498	34.868	4.4 ± 0.60	27 ± 1.7	41 ± 1.2	2.3 ± 0.23	0.65 ± 0.046	0.52 ± 0.087
100	12.404	34.856	5.6 ± 0.68	26 ± 1.8	41 ± 1.2	2.1 ± 0.21	0.64 ± 0.049	0.38 ± 0.060
C4, 176°03′ E, 43°29′ S, 387 m, 05-26-2008								
10	13.030	34.911	3.4 ± 0.19	29 ± 1.3	41 ± 1.2	3.7 ± 0.37	0.71 ± 0.037	1.1 ± 0.13
20	13.030	34.911	3.0 ± 0.21	31 ± 1.1	41 ± 1.2	2.9 ± 0.29	0.74 ± 0.035	0.95 ± 0.11
50	13.043	34.913	3.5 ± 0.20	31 ± 1.1	41 ± 1.2	3.6 ± 0.36	0.76 ± 0.035	1.0 ± 0.12
70	13.047	34.913	1.7 ± 0.15	30 ± 1.0	41 ± 1.2	2.9 ± 0.29	0.74 ± 0.032	1.7 ± 0.23
100	12.404	34.837	4.1 ± 0.23	33 ± 1.3	41 ± 1.2	1.1 ± 0.11	0.80 ± 0.041	0.27 ± 0.030
C7, 178°22′ E, 42°45′ S, 1124 m, 05-28-2008								
10	14.619	35.209	3.8 ± 0.21	31 ± 1.1	42 ± 1.3	3.3 ± 0.33	0.76 ± 0.036	0.87 ± 0.099
25	14.611	35.208	3.5 ± 0.22	31 ± 1.1	42 ± 1.3	2.9 ± 0.29	0.75 ± 0.035	0.82 ± 0.096
35	14.570	35.197	3.6 ± 0.19	31 ± 1.1	42 ± 1.3	3.1 ± 0.31	0.71 ± 0.036	0.86 ± 0.098
50	14.034	35.083	3.4 ± 0.19	29 ± 1.1	41 ± 1.2	2.9 ± 0.29	0.70 ± 0.033	0.85 ± 0.097
75	13.549	34.971	2.8 ± 0.21	31 ± 1.1	41 ± 1.2	3.4 ± 0.34	0.75 ± 0.036	1.2 ± 0.15
120	13.139	35.052	5.5 ± 0.23	35 ± 1.3	41 ± 1.2	1.9 ± 0.19	0.85 ± 0.030	0.34 ± 0.037
250	10.089	34.705	4.0 ± 0.27	35 ± 1.3	41 ± 1.2	1.6 ± 0.16	0.85 ± 0.030	0.39 ± 0.047
500	8.409	34.563	4.8 ± 0.22	33 ± 1.2	41 ± 1.2	2.1 ± 0.21	0.81 ± 0.030	0.44 ± 0.049
750	6.764	34.457	2.7 ± 0.19	40 ± 1.4	41 ± 1.2	0.76 ± 0.076	0.99 ± 0.030	0.28 ± 0.035
1090	5.123	34.436	3.7 ± 0.21	36 ± 1.2	41 ± 1.2	1.6 ± 0.16	0.89 ± 0.030	0.42 ± 0.049
C8, 178°49′ E, 42°49′ S, 1096 m, 05-29-2008								
10	14.266	35.115	3.8 ± 0.20	30 ± 1.1	41 ± 1.2	2.3 ± 0.23	0.73 ± 0.034	0.62 ± 0.071
25	14.231	35.115	3.5 ± 0.22	31 ± 0.72	41 ± 1.2	2.4 ± 0.24	0.75 ± 0.028	0.68 ± 0.081

Table 1. Continued.

Depth m	Temp. °C	Salinity	Particulate ^{234}Th mBq l^{-1}	Total ^{234}Th mBq l^{-1}	^{238}U mBq l^{-1}	POC µmol C l^{-1}	^{234}Th:^{238}U	C:Th Ratio mmol C Bq^{-1}
50	14.220	35.113	4.1 ± 0.21	34 ± 1.3	41 ± 1.2	2.2 ± 0.22	0.81 ± 0.041	0.55 ± 0.061
75	14.214	35.104	4.0 ± 0.20	30 ± 1.2	41 ± 1.2	2.3 ± 0.23	0.73 ± 0.036	0.57 ± 0.063
120	12.534	34.848	4.4 ± 0.24	34 ± 1.3	41 ± 1.2	1.2 ± 0.12	0.82 ± 0.039	0.28 ± 0.032
C9, 174°36′ E, 42°53′ S, 1010 m, 05-30-2008								
10	14.069	35.113	4.0 ± 0.21	33 ± 1.2	41 ± 1.2	2.1 ± 0.21	0.80 ± 0.038	0.53 ± 0.060
20	14.031	35.104	4.3 ± 0.23	37 ± 1.3	41 ± 1.2	2.5 ± 0.25	0.88 ± 0.040	0.57 ± 0.064
45	14.049	35.107	4.4 ± 0.21	35 ± 1.2	41 ± 1.2	1.6 ± 0.16	0.85 ± 0.039	0.36 ± 0.039
70	13.885	35.066	4.6 ± 0.20	33 ± 1.4	41 ± 1.2	1.7 ± 0.17	0.79 ± 0.040	0.38 ± 0.042
100	13.736	35.033	3.1 ± 0.20	34 ± 1.2	41 ± 1.2	2.1 ± 0.21	0.83 ± 0.038	0.69 ± 0.083
C10, 178°17′ E, 42°50′ S, 662 m, 05-31-2008								
10	14.443	35.246	2.7 ± 0.18	36 ± 1.3	42 ± 1.3	2.0 ± 0.20	0.87 ± 0.041	0.71 ± 0.085
20	14.432	35.245	3.2 ± 0.20	34 ± 1.2	42 ± 1.3	2.0 ± 0.20	0.83 ± 0.038	0.62 ± 0.073
45	14.434	35.242	3.1 ± 0.19	35 ± 1.3	42 ± 1.3	1.9 ± 0.19	0.83 ± 0.039	0.63 ± 0.074
70	14.433	35.242	3.2 ± 0.18	35 ± 1.2	42 ± 1.3	2.5 ± 0.25	0.85 ± 0.039	0.78 ± 0.089
100	14.399	35.233	3.8 ± 0.21	37 ± 1.2	42 ± 1.3	1.3 ± 0.13	0.88 ± 0.039	0.35 ± 0.041
C11, 178°42′E, 42°58′S, 528 m, 06-01-2008								
10	13.748	35.041	2.6 ± 0.17	33 ± 1.1	41 ± 1.2	3.3 ± 0.33	0.80 ± 0.035	1.3 ± 0.15
20	13.724	35.035	2.5 ± 0.19	31 ± 1.0	41 ± 1.2	2.9 ± 0.29	0.75 ± 0.033	1.2 ± 0.15
45	13.684	35.025	2.4 ± 0.17	33 ± 0.76	41 ± 1.2	2.3 ± 0.23	0.80 ± 0.030	0.94 ± 0.12
70	13.646	35.026	2.5 ± 0.17	32 ± 0.74	41 ± 1.2	2.0 ± 0.20	0.78 ± 0.030	0.80 ± 0.097
100	13.411	34.994	2.6 ± 0.19	41 ± 1.3	41 ± 1.2	1.9 ± 0.19	1.0 ± 0.043	0.73 ± 0.091
C12, 177°30′ E, 43°42′ S, 342 m, 06-02-2008								
10	13.362	35.053	1.8 ± 0.16	31 ± 1.0	41 ± 1.2	1.6 ± 0.16	0.75 ± 0.033	0.87 ± 0.12
20	13.366	35.053	2.5 ± 0.19	33 ± 0.97	41 ± 1.2	1.5 ± 0.15	0.79 ± 0.033	0.61 ± 0.076
45	13.365	35.053	2.2 ± 0.17	33 ± 1.1	41 ± 1.2	1.6 ± 0.16	0.80 ± 0.035	0.72 ± 0.090
70	13.366	35.053	2.1 ± 0.16	31 ± 1.0	41 ± 1.2	1.6 ± 0.16	0.74 ± 0.033	0.76 ± 0.097
100	13.079	35.000	3.0 ± 0.20	32 ± 1.3	41 ± 1.2	1.2 ± 0.12	0.76 ± 0.039	0.42 ± 0.050
C13, 178°31′ E, 43°42′ S, 422 m, 06-02-2008								
10	13.603	35.025	2.0 ± 0.17	34 ± 1.2	41 ± 1.2	1.9 ± 0.19	0.82 ± 0.037	0.91 ± 0.12
20	13.602	35.025	1.8 ± 0.19	35 ± 1.2	41 ± 1.2	2.1 ± 0.21	0.85 ± 0.038	1.2 ± 0.17
45	13.608	35.024	2.1 ± 0.16	34 ± 1.1	41 ± 1.2	2.6 ± 0.26	0.83 ± 0.037	1.2 ± 0.15
70	13.658	35.045	2.1 ± 0.16	32 ± 1.1	41 ± 1.2	2.0 ± 0.20	0.77 ± 0.035	0.95 ± 0.12
100	11.842	34.842	3.5 ± 0.21	39 ± 1.2	41 ± 1.2	0.98 ± 0.098	0.94 ± 0.041	0.28 ± 0.033
C21, 175°20′E, 43°68′ S, 356 m, 06-02-2008								
10	12.437	34.854	3.1 ± 0.53	29 ± 1.8	41 ± 1.2	2.4 ± 0.24	0.69 ± 0.049	0.76 ± 0.15
20	12.442	34.854	4.5 ± 0.62	31 ± 2.1	41 ± 1.2	2.7 ± 0.27	0.75 ± 0.056	0.61 ± 0.11
50	12.437	34.853	2.5 ± 0.51	36 ± 1.9	41 ± 1.2	2.5 ± 0.25	0.87 ± 0.052	1.0 ± 0.23
70	12.438	34.853	4.3 ± 0.51	33 ± 1.9	41 ± 1.2	2.3 ± 0.23	0.81 ± 0.051	0.54 ± 0.083
100	12.419	34.850	4.5 ± 0.62	37 ± 2.0	41 ± 1.2	2.4 ± 0.24	0.89 ± 0.055	0.52 ± 0.088
Mid-Salinity Stations								
C5, 176°30′ E, 43°39′ S, 367 m, 05-27-2008								
10	11.433	34.481	7.6 ± 0.26	33 ± 1.2	41 ± 1.2	5.2 ± 0.52	0.80 ± 0.037	0.68 ± 0.072
20	11.433	34.480	9.3 ± 0.29	31 ± 1.2	41 ± 1.2	5.6 ± 0.56	0.76 ± 0.037	0.60 ± 0.063
50	11.647	34.536	6.6 ± 0.24	33 ± 1.2	41 ± 1.2	4.1 ± 0.41	0.82 ± 0.039	0.63 ± 0.067
70	11.547	34.616	5.5 ± 0.23	35 ± 1.3	41 ± 1.2	3.6 ± 0.36	0.86 ± 0.041	0.65 ± 0.071
100	10.886	34.701	3.0 ± 0.21	35 ± 1.3	41 ± 1.2	1.2 ± 0.12	0.85 ± 0.040	0.39 ± 0.048

Table 1. Continued.

Depth m	Temp. °C	Salinity	Particulate ^{234}Th mBq l^{-1}	Total ^{234}Th mBq l^{-1}	^{238}U mBq l^{-1}	POC µmol C l^{-1}	^{234}Th:^{238}U	C:Th Ratio mmol C Bq^{-1}
150	10.467	34.727	3.8 ± 0.21	36 ± 1.2	41 ± 1.2	1.3 ± 0.13	0.87 ± 0.039	0.36 ± 0.041
250	9.539	34.664	3.9 ± 0.21	33 ± 1.2	41 ± 1.2	0.96 ± 0.096	0.82 ± 0.039	0.24 ± 0.028
340	8.930	34.606	5.8 ± 0.23	31 ± 1.3	41 ± 1.2	1.9 ± 0.19	0.75 ± 0.039	0.33 ± 0.035
C6, 178°22′ E, 43°02′ S, 340 m, 05-28-2008								
10	11.660	34.536	8.8 ± 0.27	27 ± 0.92	41 ± 1.2	6.1 ± 0.61	0.65 ± 0.030	0.69 ± 0.073
20	11.664	34.536	9.1 ± 0.29	29 ± 1.1	41 ± 1.2	5.7 ± 0.57	0.72 ± 0.034	0.63 ± 0.066
50	11.672	34.538	9.5 ± 0.28	30 ± 1.1	41 ± 1.2	6.1 ± 0.61	0.74 ± 0.034	0.64 ± 0.067
70	11.679	34.544	9.1 ± 0.27	30 ± 1.2	41 ± 1.2	5.4 ± 0.54	0.73 ± 0.037	0.59 ± 0.062
100	11.247	34.740	3.3 ± 0.21	33 ± 1.1	41 ± 1.2	1.8 ± 0.18	0.80 ± 0.035	0.54 ± 0.064
150	10.601	34.728	3.1 ± 0.20	35 ± 2.6	41 ± 1.2	1.1 ± 0.11	0.86 ± 0.068	0.35 ± 0.042
250	8.966	34.605	1.8 ± 0.17	35 ± 1.3	41 ± 1.2	0.40 ± 0.040	0.86 ± 0.040	0.22 ± 0.031
315	8.452	34.546	5.4 ± 0.24	24 ± 1.0	41 ± 1.2	1.6 ± 0.16	0.60 ± 0.030	0.29 ± 0.031
C14, 178°20′ E, 44°14′ S, 526 m, 06-03-2008								
10	10.837	34.340	11 ± 0.29	29 ± 1.2	41 ± 1.2	3.6 ± 0.36	0.72 ± 0.036	0.32 ± 0.033
20	10.858	34.344	11 ± 0.30	32 ± 1.0	41 ± 1.2	2.0 ± 0.20	0.79 ± 0.034	0.18 ± 0.018
45	11.021	34.390	12 ± 0.29	33 ± 1.1	41 ± 1.2	3.7 ± 0.37	0.82 ± 0.036	0.32 ± 0.033
70	11.099	34.438	11 ± 0.28	32 ± 1.1	41 ± 1.2	3.3 ± 0.33	0.79 ± 0.036	0.31 ± 0.032
100	10.485	34.578	3.5 ± 0.21	37 ± 1.1	41 ± 1.2	1.1 ± 0.11	0.90 ± 0.038	0.32 ± 0.037
150	10.485	34.590	n.d.	40 ± 1.3	41 ± 1.2	0.79 ± 0.079	0.98 ± 0.044	n.d.
C15, 177°48′ E, 44°24′ S, 716 m, 06-03-2008								
10	11.109	34.386	11 ± 0.31	32 ± 1.2	41 ± 1.2	4.7 ± 0.47	0.80 ± 0.038	0.41 ± 0.042
20	11.096	34.383	12 ± 0.32	28 ± 1.1	41 ± 1.2	4.4 ± 0.44	0.69 ± 0.033	0.38 ± 0.039
50	10.905	34.353	7.2 ± 0.26	33 ± 1.2	41 ± 1.2	2.3 ± 0.23	0.81 ± 0.038	0.32 ± 0.034
70	11.029	34.416	6.8 ± 0.24	38 ± 1.4	41 ± 1.2	1.7 ± 0.17	0.93 ± 0.045	0.26 ± 0.027
100	10.879	34.626	2.8 ± 0.21	39 ± 1.3	41 ± 1.2	0.88 ± 0.088	0.96 ± 0.043	0.31 ± 0.038
C16, 178°28′ E, 44°33′ S, 1078 m, 06-04-2008								
10	10.361	34.265	11 ± 0.30	29 ± 1.1	40 ± 1.2	4.1 ± 0.41	0.72 ± 0.036	0.37 ± 0.038
20	10.380	34.270	11 ± 0.31	29 ± 1.2	40 ± 1.2	3.6 ± 0.36	0.72 ± 0.036	0.33 ± 0.034
40	10.409	34.277	9.1 ± 0.28	31 ± 1.1	40 ± 1.2	3.7 ± 0.37	0.76 ± 0.035	0.40 ± 0.042
65	10.824	34.465	7.7 ± 0.25	29 ± 1.0	41 ± 1.2	2.3 ± 0.23	0.71 ± 0.033	0.30 ± 0.032
100	9.767	34.531	3.8 ± 0.22	40 ± 1.3	41 ± 1.2	1.3 ± 0.13	0.98 ± 0.044	0.33 ± 0.039
C20, 178°22′ E, 43°37′ S, 364 m, 06-06-2008								
10	11.234	34.579	5.9 ± 0.61	35 ± 2.1	41 ± 1.2	4.1 ± 0.41	0.86 ± 0.058	0.69 ± 0.099
20	11.235	34.579	5.2 ± 0.71	31 ± 2.1	41 ± 1.2	4.7 ± 0.47	0.76 ± 0.056	0.89 ± 0.15
50	11.224	34.579	8.4 ± 0.63	36 ± 2.3	41 ± 1.2	4.2 ± 0.42	0.89 ± 0.061	0.50 ± 0.062
70	11.223	34.579	6.5 ± 0.58	34 ± 2.8	41 ± 1.2	4.0 ± 0.40	0.82 ± 0.073	0.61 ± 0.081
120	11.137	34.641	5.8 ± 0.68	35 ± 2.3	41 ± 1.2	2.9 ± 0.29	0.86 ± 0.061	0.50 ± 0.076
250	9.409	34.608	6.1 ± 0.61	42 ± 2.4	41 ± 1.2	0.92 ± 0.092	1.1 ± 0.066	0.15 ± 0.021
350	8.890	34.585	5.9 ± 0.66	31 ± 2.3	41 ± 1.2	1.3 ± 0.13	0.76 ± 0.062	0.23 ± 0.034
C22, 175°20′E, 43°99′S, 470 m, 06-10-2008								
10	10.870	34.593	5.5 ± 0.58	35 ± 2.0	41 ± 1.2	4.1 ± 0.41	0.85 ± 0.056	0.75 ± 0.11
20	10.880	34.595	4.9 ± 0.64	36 ± 2.3	41 ± 1.2	4.0 ± 0.40	0.89 ± 0.063	0.82 ± 0.14
50	10.811	34.581	6.8 ± 0.60	36 ± 2.1	41 ± 1.2	4.6 ± 0.46	0.89 ± 0.058	0.67 ± 0.090
70	10.732	34.567	6.2 ± 0.54	34 ± 2.1	41 ± 1.2	3.3 ± 0.33	0.84 ± 0.057	0.53 ± 0.071
100	10.689	34.565	5.5 ± 0.69	33 ± 1.9	41 ± 1.2	3.2 ± 0.32	0.80 ± 0.053	0.57 ± 0.091
D1, 174°65′ E, 43°65′ S, 510 m, 06-10-2008								
10	9.928	34.443	4.9 ± 0.58	32 ± 2.0	41 ± 1.2	4.2 ± 0.42	0.80 ± 0.056	0.84 ± 0.13

Table 1. Continued.

Depth m	Temp. °C	Salinity	Particulate ^{234}Th mBq l^{-1}	Total ^{234}Th mBq l^{-1}	^{238}U mBq l^{-1}	POC µmol C l^{-1}	^{234}Th:^{238}U	C:Th Ratio mmol C Bq^{-1}
20	9.980	34.451	4.6 ± 0.69	32 ± 2.3	41 ± 1.2	4.3 ± 0.43	0.78 ± 0.061	0.95 ± 0.17
50	10.005	34.455	4.8 ± 0.58	29 ± 2.0	41 ± 1.2	4.0 ± 0.40	0.71 ± 0.053	0.85 ± 0.13
70	9.966	34.448	4.8 ± 0.56	33 ± 2.1	41 ± 1.2	4.1 ± 0.41	0.82 ± 0.058	0.86 ± 0.13
100	9.945	34.452	4.6 ± 0.64	37 ± 2.1	41 ± 1.2	2.3 ± 0.23	0.91 ± 0.058	0.50 ± 0.087
C4-2[b], 06-07-2008								
10	10.975	34.542	7.9 ± 0.73	37 ± 2.2	41 ± 1.2	5.6 ± 0.56	0.90 ± 0.059	0.71 ± 0.097
20	10.975	34.542	7.3 ± 0.78	39 ± 2.5	41 ± 1.2	5.3 ± 0.53	0.95 ± 0.067	0.72 ± 0.11
50	10.979	34.542	8.1 ± 0.66	24 ± 3.0	41 ± 1.2	5.2 ± 0.52	0.59 ± 0.075	0.64 ± 0.083
70	10.981	34.542	7.2 ± 0.65	31 ± 2.2	41 ± 1.2	5.2 ± 0.52	0.76 ± 0.059	0.73 ± 0.099
100	10.980	34.543	8.5 ± 0.79	35 ± 2.4	41 ± 1.2	5.6 ± 0.56	0.85 ± 0.065	0.66 ± 0.090
Low Salinity Stations								
C17,178°35′ E, 44°21′ S, 1186 m, 06-05-2008								
10	9.699	34.206	7.8 ± 0.26	27 ± 1.0	40 ± 1.2	3.1 ± 0.31	0.66 ± 0.032	0.40 ± 0.042
20	9.698	34.206	9.5 ± 0.76	30 ± 1.1	40 ± 1.2	2.4 ± 0.24	0.74 ± 0.036	0.26 ± 0.033
C22, 175°20′ E, 43°99′ S, 470 m, 06-10-2008								
45	9.704	34.206	7.5 ± 0.25	28 ± 1.0	40 ± 1.2	2.3 ± 0.23	0.68 ± 0.033	0.31 ± 0.033
65	9.686	34.209	4.1 ± 0.20	32 ± 1.1	40 ± 1.2	1.5 ± 0.15	0.79 ± 0.036	0.35 ± 0.039
100	9.363	34.383	3.5 ± 0.22	38 ± 1.3	41 ± 1.2	1.4 ± 0.14	0.94 ± 0.043	0.39 ± 0.046
250	7.635	34.422	3.1 ± 0.20	39 ± 1.3	41 ± 1.2	1.0 ± 0.10	0.96 ± 0.043	0.33 ± 0.040
500	6.843	34.370	3.7 ± 0.21	36 ± 1.2	41 ± 1.2	1.2 ± 0.12	0.89 ± 0.041	0.33 ± 0.037
750	5.563	34.291	4.0 ± 0.20	36 ± 1.2	40 ± 1.2	0.61 ± 0.061	0.90 ± 0.040	0.15 ± 0.017
1170	3.253	34.380	6.0 ± 0.26	31 ± 1.1	41 ± 1.2	1.0 ± 0.10	0.78 ± 0.036	0.17 ± 0.019
C18, 177°43′ E, 44°06′ S, 942 m, 06-05-2008								
10	9.699	34.237	7.2 ± 0.26	31 ± 1.0	40 ± 1.2	4.0 ± 0.40	0.77 ± 0.034	0.56 ± 0.059
20	9.705	34.239	7.3 ± 0.27	31 ± 1.0	40 ± 1.2	3.9 ± 0.39	0.76 ± 0.035	0.54 ± 0.057
45	9.715	34.241	7.7 ± 0.26	31 ± 1.1	40 ± 1.2	3.8 ± 0.38	0.76 ± 0.035	0.50 ± 0.052
65	9.974	34.349	4.9 ± 0.22	36 ± 1.2	41 ± 1.2	2.8 ± 0.28	0.88 ± 0.040	0.57 ± 0.062
100	9.768	34.464	2.8 ± 0.21	35 ± 1.2	41 ± 1.2	1.1 ± 0.11	0.86 ± 0.039	0.38 ± 0.048
250	8.046	34.463	3.8 ± 0.22	38 ± 1.3	41 ± 1.2	0.90 ± 0.090	0.94 ± 0.042	0.24 ± 0.028
500	7.013	34.384	2.6 ± 0.19	39 ± 1.3	41 ± 1.2	1.1 ± 0.11	0.96 ± 0.043	0.41 ± 0.051
750	5.990	34.312	4.1 ± 0.21	37 ± 1.2	40 ± 1.2	0.74 ± 0.074	0.91 ± 0.041	0.18 ± 0.020
890	5.553	34.290	4.7 ± 0.40	35 ± 1.2	40 ± 1.2	1.4 ± 0.014	0.87 ± 0.040	0.30 ± 0.040
C23, 175°17′ E, 44°23′ S, 653 m, 06-08-2008								
10	9.443	34.252	7.3 ± 0.67	35 ± 2.2	40 ± 1.2	3.7 ± 0.37	0.86 ± 0.061	0.50 ± 0.069
20	9.436	34.250	5.3 ± 0.74	33 ± 2.9	40 ± 1.2	3.5 ± 0.35	0.81 ± 0.076	0.66 ± 0.11
40	9.441	34.251	7.0 ± 0.63	33 ± 2.9	40 ± 1.2	3.4 ± 0.34	0.80 ± 0.061	0.48 ± 0.064
60	9.497	34.270	5.4 ± 0.60	34 ± 2.3	40 ± 1.2	3.0 ± 0.30	0.84 ± 0.061	0.56 ± 0.083
80	9.646	34.371	7.5 ± 0.72	32 ± 2.2	41 ± 1.2	3.0 ± 0.30	0.78 ± 0.059	0.40 ± 0.055

a, b: second visits at Station C3 and C4.

3.4 ^{234}Th export flux estimates

The export flux of ^{234}Th at a specific depth horizon can be estimated by using the following equation:

$$\frac{\delta A_{\mathrm{Th}}}{\delta t} = A_{\mathrm{U}}\lambda_{\mathrm{Th}} - A_{\mathrm{Th}}\lambda_{\mathrm{Th}} - P + V \quad (1)$$

where $\frac{\delta A_{\mathrm{Th}}}{\delta t}$ is the rate of change of total ^{234}Th activity, A_{U} is the ^{238}U activity estimated from the U-S relationship (Chen et al., 1986), A_{Th} is the total ^{234}Th activity, λ_{Th} is the decay constant for ^{234}Th (0.02876 d^{-1}), P is the net removal flux of ^{234}Th on particles, and V is the sum of contributions from advection and diffusion.

Table 2. Inventories of dissolved inorganic nitrogen (DIN), $Si(OH)_4$, particulate organic carbon (POC), particulate ^{234}Th and Chl-*a*, Steady-State (SS) ^{234}Th flux, POC/^{234}Th ratios and POC flux in the upper 100 m and euphotic zone (Ez) within the Subtropical Front in May–June 2008.

Station	Euphotic Zone[a] (Ez) m	DIN 0–100 m $\times 10^2$ mmol m^{-2}	$Si(OH)_4$ 0–100 m $\times 10^2$ mmol m^{-2}	POC, 0–100 m $\times 10^2$ mmolC m^{-2}	Part.^{234}Th, 0–100 m $\times 10^2$ Bq m^{-2}	Chl-*a*, 0–100 m mg m^{-2}	Chl-*a*, 0-Ez bottom mg m^{-2}	SS ^{234}Th flux @100 m Bq m^{-2}d^{-1}	SS ^{234}Th flux @Ez[b] Bq m^{-2} d^{-1}	C/Th Ratio[c] mmol C Bq^{-1}	POC Flux @100 m mmol C m^{-2}d^{-1}
High Salinity Stations											
C1	160	5.0	2.4	2.8 ± 0.064	2.9 ± 0.068	43 ± 0.43	55 ± 0.47	43 ± 1.7	57 ± 2.4	0.70 ± 0.081	30 ± 3.7
C2	170	2.5	2.0	3.4 ± 0.10	4.7 ± 0.078	49 ± 0.52	60 ± 0.53	32 ± 1.8	42 ± 2.8	0.46 ± 0.051	15 ± 1.8
C3	100	5.9	1.8	2.6 ± 0.053	2.5 ± 0.068	37 ± 0.38	37 ± 0.38	36 ± 1.7	36 ± 1.7	0.82 ± 0.11	29 ± 4.0
C3-2	100	n.d	n.d	2.1 ± 0.092	4.2 ± 0.23	25 ± 0.26	25 ± 0.26	44 ± 2.4	44 ± 2.4	0.38 ± 0.060	17 ± 2.8
C4	110	6.2	2.0	2.9 ± 0.068	3.0 ± 0.071	63 ± 0.65	63 ± 0.65	29 ± 1.7	31 ± 1.8	0.27 ± 0.030	7.8 ± 1.0
C7	130	4.3	n.d	3.5 ± 0.10	4.4 ± 0.090	48 ± 0.50	52 ± 0.51	34 ± 2.1	34 ± 2.1	0.34 ± 0.037	12 ± 1.5
C8	130	4.0	n.d	2.5 ± 0.11	4.7 ± 0.094	44 ± 0.45	47 ± 0.45	33 ± 2.2	34 ± 2.2	0.28 ± 0.032	9.4 ± 1.2
C9	160	3.6	n.d	2.0 ± 0.089	4.2 ± 0.075	35 ± 0.35	51 ± 0.42	20 ± 1.8	26 ± 2.6	0.69 ± 0.083	14 ± 2.1
C10	150	3.0	n.d	2.0 ± 0.070	3.2 ± 0.069	40 ± 0.40	54 ± 0.46	18 ± 1.8	22 ± 2.4	0.35 ± 0.041	6.5 ± 0.98
C11	140	6.0	n.d	2.4 ± 0.053	2.5 ± 0.064	25 ± 0.25	28 ± 0.26	22 ± 1.6	22 ± 1.6	0.73 ± 0.091	16 ± 2.3
C12	150	5.9	n.d	1.5 ± 0.051	2.3 ± 0.063	50 ± 0.51	56 ± 0.52	27 ± 1.7	34 ± 2.3	0.42 ± 0.050	11 ± 1.5
C13	100	4.7	n.d	2.0 ± 0.050	2.2 ± 0.063	35 ± 0.38	35 ± 0.38	20 ± 1.7	20 ± 1.7	0.28 ± 0.033	5.6 ± 0.81
C21	200	7.6	n.d	2.5 ± 0.085	3.8 ± 0.20	32 ± 0.33	60 ± 0.44	22 ± 2.4	29 ± 4.5	0.52 ± 0.088	12 ± 2.3
Mid-Salinity Stations											
C5	100	7.8	1.6	4.0 ± 0.15	6.6 ± 0.089	83 ± 0.97	83 ± 0.97	21 ± 1.8	21 ± 1.8	0.39 ± 0.048	8.4 ± 1.3
C6	100	7.5	1.2	5.2 ± 0.18	8.3 ± 0.097	92 ± 1.0	92 ± 1.0	31 ± 1.7	31 ± 1.7	0.54 ± 0.064	17 ± 2.2
C14	100	10.8	n.d	2.8 ± 0.22	9.9 ± 0.099	58 ± 0.66	58 ± 0.66	22 ± 1.7	22 ± 1.7	0.32 ± 0.037	7.0 ± 0.97
C15	100	8.8	n.d	2.7 ± 0.18	8.0 ± 0.096	59 ± 0.69	59 ± 0.69	19 ± 1.8	19 ± 1.8	0.31 ± 0.038	6.0 ± 0.93
C16	100	10.6	n.d	2.9 ± 0.18	8.3 ± 0.096	60 ± 0.75	60 ± 0.75	27 ± 1.8	27 ± 1.8	0.33 ± 0.039	8.9 ± 0.7
C20	160	8.4	n.d	4.7 ± 0.18	7.7 ± 0.29	88 ± 0.90	96 ± 0.92	23 ± 3.6	24 ± 3.6	0.50 ± 0.076	11 ± 2.5
C22	150	9.9	n.d	3.9 ± 0.13	5.9 ± 0.22	87 ± 0.87	101 ± 0.90	17 ± 2.5	23 ± 3.4	0.57 ± 0.091	9.4 ± 2.1
D1	140	n.d	n.d	3.9 ± 0.10	4.7 ± 0.22	63 ± 0.64	72 ± 0.66	24 ± 2.5	26 ± 3.0	0.50 ± 0.087	12 ± 2.5
C4-2	150	n.d	n.d	5.3 ± 0.17	7.7 ± 0.26	128 ± 1.3	153 ± 1.4	24 ± 2.9	29 ± 3.6	0.66 ± 0.090	16 ± 2.9
Low Salinity Stations											
C17	120	9.9	n.d	2.0 ± 0.14	6.3 ± 0.14	36 ± 0.41	37 ± 0.42	27 ± 1.7	27 ± 1.8	0.39 ± 0.046	10 ± 1.4
C18	130	11.2	n.d	3.1 ± 0.13	5.9 ± 0.088	39 ± 0.44	41 ± 0.44	22 ± 1.7	23 ± 1.8	0.38 ± 0.048	8.3 ± 1.2
C23	150	8.0	n.d	2.6 ± 0.11	5.0 ± 0.19	35 ± 0.36	39 ± 0.37	17 ± 2.2	25 ± 3.6	0.40 ± 0.055	6.7 ± 1.3

n.d: not determined

[a] The depth of euphotic zone (Ez) is estimated to be where fluorescence reaches its minimum.

[b] For those stations where Ez > 100 m, ^{234}Th was assumed to be in equilibrium with dissolved ^{238}U at the base of the Ez as most of the stations were only sampled in the upper 100 m, and ^{234}Th flux was then integrated down to the base of the Ez.

[c] Bottle C/Th ratios@100 m are used in these calculations, such that the estimated POC fluxes should be considered as upper limits for the Chatham Rise region at the time of sampling.

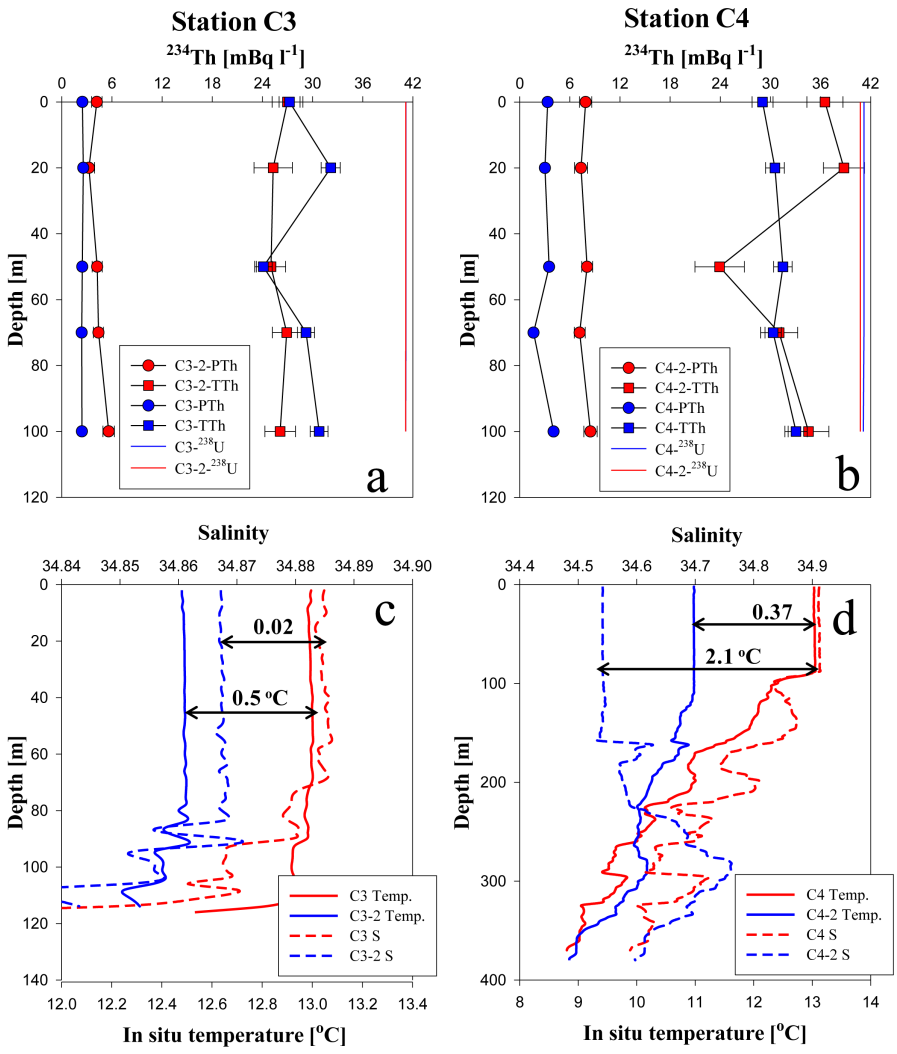

Fig. 7. **(a)** and **(b)** Vertical distributions of particulate and total ^{234}Th during the two visits to stations C3 and C4, with 16 days between C3 (26 May) and C3-2 (11 June) and 12 days between C4 (26 May) and C4-2 (7 June). **(c)** and **(d)** Vertical distributions of temperature and salinity at C3 and C4.

The Steady State (SS) model is applicable when little temporal change ($\frac{\delta A_{\mathrm{Th}}}{\delta t}$) occurs in ^{234}Th activities or SS ^{234}Th flux is low (Savoye et al., 2006). However, when there are rapid changes in ^{234}Th activities, for example, during algal blooms or within physically dynamic regions, such as the STF, a non-steady state (NSS) ^{234}Th flux model is generally necessary (Buesseler et al., 1992). To implement a NSS ^{234}Th flux model, however, time-series observations from the same water mass are needed. In a practical sense, since there are difficulties in tracing specific water masses in the ocean, most studies have adopted a protocol to visit the same station at least twice during a particular study period (Benitez-Nelson et al., 2001b; Coppola et al., 2005; Kawakami and Honda, 2007). NSS ^{234}Th flux can then be calculated using the following equation (Buesseler et al., 1992):

$$P_{\mathrm{NSS}} = \frac{\lambda[A_{\mathrm{U}}(1-e^{-\lambda t}) + A_{\mathrm{Th1}}e^{-\lambda t} - A_{\mathrm{Th2}}]}{1-e^{-\lambda t}} \quad (2)$$

where P_{NSS} is the NSS ^{234}Th export flux, and A_{Th1} and A_{Th2} are the ^{234}Th activities during the first and second visit, respectively. During our cruise, two stations (C3 and C4) were visited twice. The profiles of the temperature, salinity and ^{234}Th activity for these stations are shown in Fig. 7. At C3, differences in temperature and salinity of the upper 100 m between the two visits were 0.5 °C and 0.02, respectively. In contrast, at C4, larger differences were found: 2.1 °C for temperature and 0.37 for salinity, which clearly indicated that different water masses were present at this location between the two visits. Due to the relatively minor changes in hydrography, however, we assume the same water mass was

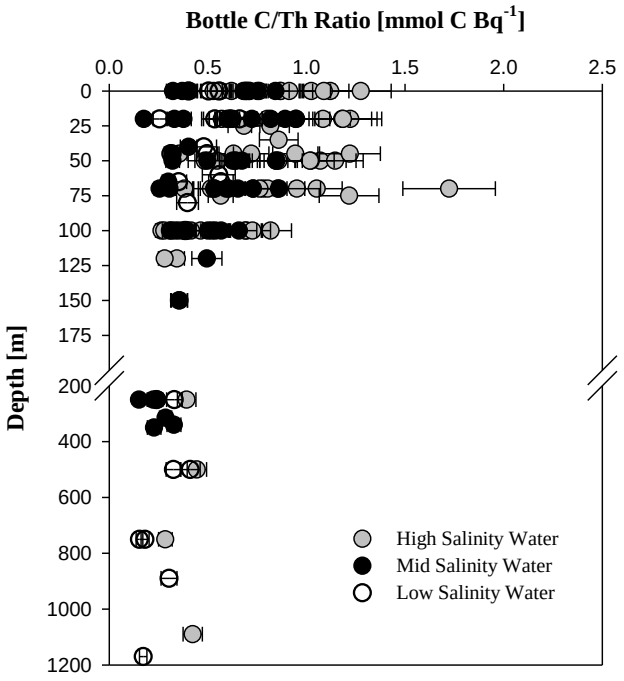

Fig. 8. Profiles of bottled POC/Th ratios for the three water types identified by their salinity differences (see Fig. 2).

sampled during the two visits to C3. Given the potential influence from the bottom re-suspension at this shallow station (see later), NSS ^{234}Th flux from the upper 10 m was calculated as 4.1 Bq m^{-2} d^{-1}. The SS ^{234}Th fluxes from the upper 10 m for the two visits to C3 were 4.0 and 4.1 Bq m^{-2} d^{-1}, indicating that there was little temporal variability of ^{234}Th flux at this location. As such, the SS model is regarded to be mostly suitable for our ^{234}Th flux calculations for all the other locations sampled in the STF.

Physical processes may also influence the estimates of downward ^{234}Th fluxes. Previous studies indicate that currents over the Chatham Rise can be strong, but variable, with alternating zones of convergence and divergence, although net zonal flows dominate along the northern and southern edges of Chatham Rise and predominantly meridional flows occur over the rise itself (Chiswell, 1996; Sutton, 2001). Given the little change observed in total ^{234}Th activities along the salinity gradients as shown in Fig. 6, however, we assumed that the horizontal contribution to the ^{234}Th fluxes was small compared to the downward vertical component of ^{234}Th export. Therefore, the V term in Eq. (3) can be neglected in our ^{234}Th flux estimates.

Based on the above discussion, the P term in Eq. (1) can then be solved as follows:

$$P = \lambda_{\mathrm{Th}}(A_{\mathrm{U}} - A_{\mathrm{Th}}) \quad (3)$$

In our case, the steady state (SS) downward flux of total ^{234}Th from the depth horizon of 100 m can be integrated by:

$$P = \lambda_{\mathrm{Th}} \int_0^{100} (A_{\mathrm{U}} - A_{\mathrm{Th}}) dz \quad (4)$$

The calculated ^{234}Th flux results for the upper 100 m of the water column are listed in Table 2. SS ^{234}Th fluxes range from 17 ± 2.2 Bq m^{-2} d^{-1} to a maximum of 43 ± 1.7 Bq m^{-2} d^{-1}, with an average of 26 ± 0.41 Bq m^{-2} d^{-1} ($n = 25$). It is noted, however, that the highest value is from Station C3 with a bottom depth of 125 m, and which consequently may be influenced by near-bottom re-suspension. As discussed previously, we also separated our ^{234}Th flux data into three groups. In low salinity waters, SS ^{234}Th fluxes varied from 17 ± 2.2 Bq m^{-2} d^{-1}to 27 ± 1.7 Bq m^{-2} d^{-1}, with an average of 22 ± 1.1 Bq m^{-2} d^{-1} ($n = 3$). In mid-salinity waters, the flux varied from 17 ± 2.5 Bq m^{-2} d^{-1} to 31 ± 1.7 Bq m^{-2} d^{-1}, with an average of 25 ± 0.78 Bq m^{-2} d^{-1} ($n = 9$). In high salinity waters, SS ^{234}Th fluxes were similar to those in mid-salinity waters, namely, 18 ± 1.1 Bq m^{-2} d^{-1}to 44 ± 2.4 Bq m^{-2} d^{-1}, with an average of 29 ± 0.53 Bq m^{-2} d^{-1} ($n = 13$).

3.5 Bottle POC/^{234}Th ratios

Bottle POC/^{234}Th ratios are listed in Table 1. This ratio was quite variable, ranging from 0.15 mmol C Bq^{-1} to 1.7 mmol C Bq^{-1}. All POC/^{234}Th ratios were separated into three groups based on the previously defined salinity criteria, as shown in Fig. 8. Consistent with many prior studies, POC/^{234}Th was higher and more variable in the upper ocean, compared to the deep ocean (Buesseler et al., 2006). Interestingly, the ratio was generally lower in mid- and low salinity waters than in high salinity waters, reflecting different biological effects on carbon and thorium partitioning. This difference disappeared at and below 100 m. At the export horizon of 100 m, bottle POC/^{234}Th ratios varied from 0.27 ± 0.030 mmol C Bq^{-1} to 0.82 ± 0.11 mmol C Bq^{-1}, with an average of 0.46 ± 0.013 mmol C Bq^{-1} (Table 1). Similar to ^{234}Th fluxes, no difference in POC/^{234}Th ratio was found among the three water types. In high salinity waters, the POC/^{234}Th ratio ranged from 0.27 ± 0.030 mmol C Bq^{-1} to 0.82 ± 0.11 mmol C Bq^{-1}, with an average of 0.48 ± 0.018 mmol C Bq^{-1}. In mid-salinity waters, it varied from 0.31 ± 0.038 mmol C Bq^{-1} to 0.66 ± 0.090 mmol C Bq^{-1}, with an average of 0.66 ± 0.022 mmol C Bq^{-1}. In low salinity waters, POC/^{234}Th was less variable, ranging from 0.38 ± 0.048 mmol C Bq^{-1} to 0.40 ± 0.055 mmol C Bq^{-1}, with an average of 0.39 ± 0.029 mmol C Bq^{-1}.

4 Discussion

4.1 POC/^{234}Th ratios and POC export flux

POC export fluxes can be estimated by multiplying ^{234}Th fluxes by the POC/^{234}Th ratios of sinking particles (Buesseler et al., 1992). To better constrain the POC export from the upper ocean using the ^{234}Th method, knowledge of the POC/^{234}Th ratios in sinking particles should be examined. However, in the present study, only bottle POC/^{234}Th data were collected during the cruise.

Many studies have shown that the bottle POC/^{234}Th ratio is typically higher than in pump and trap samples (Buesseler et al., 2006; Cai et al., 2008; Kawakami and Honda, 2007). Although bottle POC/^{234}Th ratios from particles in bottle samples are not expected to be particularly representative of sinking particles, it is reasonable to apply these measurements as an upper limit for the actual POC/^{234}Th ratio in sinking particles (Cai et al., 2008). A major advantage of this approach is that bottle filtrations enabled us to undertake high spatial resolution sampling of POC/^{234}Th, compared to the spatially limited deployment of in situ pumps and sediment traps.

POC export fluxes estimated from SS ^{234}Th flux and bottle POC/^{234}Th ratios at the export depth horizon of 100 m are listed in Table 2. POC export ranged from 5.6 ± 0.81 to 30 ± 3.7 mmol C m^{-2} d^{-1}, with an average of 12 ± 0.41 mmol C m^{-2} d^{-1} ($n = 25$). As expected, POC export fluxes were similar among all three water types, which is in good agreement with the ^{234}Th flux distributions. POC flux varied from 5.6 ± 0.81 mmol C m^{-2} d^{-1} to 30 ± 3.7 mmol C m^{-2} d^{-1} in high salinity waters, with an average of 14 ± 0.62 mmol C m^{-2} d^{-1} ($n = 13$), and from 6.7 ± 1.3 mmol C m^{-2} d^{-1} to 10 ± 1.4 mmol C m^{-2} d^{-1} in low salinity waters, with an average of 8.5 ± 0.75 mmol C m^{-2} d^{-1} (n=3). In comparison, POC flux ranged from 6.0 ± 0.93 mmol C m^{-2} d^{-1} to 17 ± 2.2 mmol C m^{-2} d^{-1} in mid-salinity waters, with an average of 11 ± 0.65 mmol C m^{-2} d^{-1} ($n = 9$).

Due to the lack of an effective methodology for determining downward POC export in such a physically dynamic area, few similar studies have been carried out in the STF over the Chatham Rise or even in other STF zones globally. Nodder (1997) attempted to test the hypothesis that the STF is a region of elevated export production in austral autumn via the deployment of a free-floating, surface-tethered, cylindrical sediment trap array on the northern side of the Chatham Rise. Mean POC fluxes were estimated to be $\sim$2.5 mmol C m^{-2} d^{-1} at 200 m water depth, which is similar in magnitude to other locations in oligotrophic waters. Nodder and Alexander (1998) showed that spring particulate phosphorus fluxes at $\sim$100 m in the STF were almost double those in winter 1993. These earlier studies, however, were limited in their spatial coverage, which restricts the reliability of these results when extrapolated to the entire STF. Long-term moored sediment traps were deployed for a year at 300 m and 1000 m in the STF on the flanks of the Chatham Rise to investigate the seasonal variation of particle fluxes (Nodder and Northcote, 2001). POC export reached its maximum in spring (14.8 mmol C m^{-2} d^{-1} at 300 m in the North and 4.8 mmol C m^{-2} d^{-1} in the South), and annual average POC fluxes were calculated to be 10.1 mmol C m^{-2} d^{-1} in the North, compared to 4.1 mmol C m^{-2} d^{-1} in the South. POC export was also determined in frontal zones (including the STF and Polar Front) in the Indian Ocean sector of the Southern Ocean in summer using ^{234}Th methods (Coppola et al., 2005). At an export depth horizon of 100 m, POC export varied from 0.1 to 2.5 mmol C m^{-2} d^{-1}, which is very low compared to other observations in the Southern Ocean (Buesseler et al., 2001b; Rutgers van der Loeff et al., 1997, 2002). The low diatom dominance in the water column was hypothesized to result in these lower than expected export fluxes. However, direct comparisons between these studies are difficult due to differences in the regional oceanography, observation duration, the chosen export depth horizon and applied methodologies. The export fluxes presented here for the STF on the Chatham Rise, are also only applicable to the season in which they were collected (i.e. late autumn–early winter), and it is expected that POC fluxes in the highly productive spring might be significantly enhanced in comparison (Nodder and Alexander, 1998; Nodder and Northcote, 2001). Nevertheless, the calculated POC fluxes using the ^{234}Th method are at least similar in magnitude to previous measurements of POC export in the same area, and provide us with the first appreciation of the substantial degree of spatial variability that could be expected in POC flux to the seafloor on the Chatham Rise. The POC flux estimated at 100 m in the present study decreased from west to east and from north to south across the rise (Fig. 9f). Benthic biomass and activity is generally higher on the southern flank of the Chatham Rise, compared to the crest and northern flank (Nodder et al., 2003, 2007; Probert and McKnight, 1993), which is somewhat incongruous with the lower POC fluxes suggested by this study and previous sediment trap results (Nodder and Northcote, 2001). Thus, it might be the quality, rather than the quantity, of POC supply to the benthos that has the most influence in structuring seafloor communities in this region (Nodder et al., 2003, 2007).

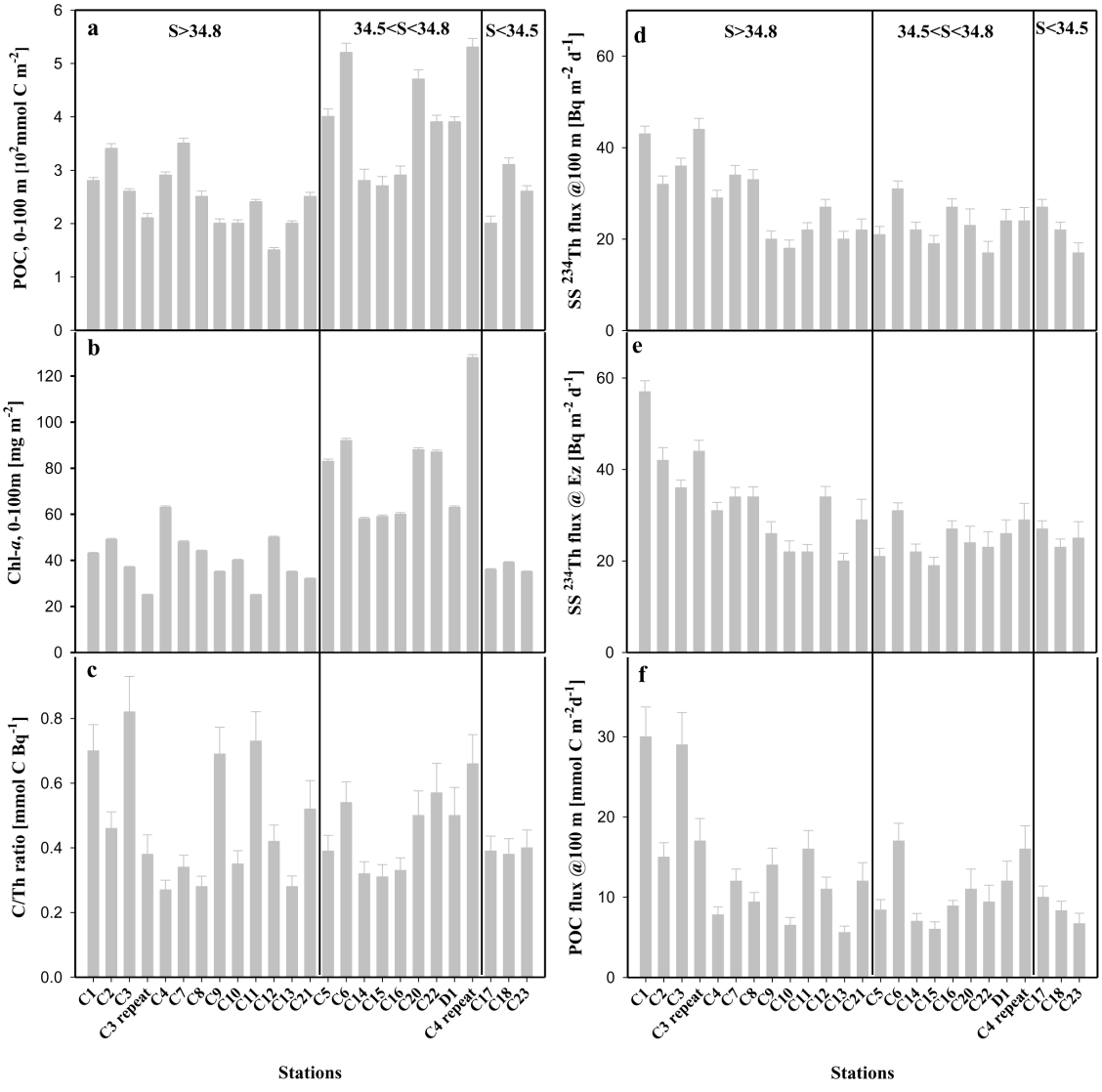

Fig. 9. Spatial distributions of: **(a)** POC inventory from 0–100 m, **(b)** Chl-*a* inventory from 0–100 m, **(c)** POC/Th ratio at 100 m, **(d)** ^{234}Th fluxes at 100 m, **(e)** ^{234}Th fluxes at the base of the Ez, and **(f)** POC fluxes at 100 m. All stations are separated into three water types: low salinity (S < 34.5), mid-salinity (34.5 < S < 34.8), and high salinity (S > 34.8) waters.

Table 3. *P* values derived from t-tests with unequal variance on inventories of POC, Particulate ^{234}Th and Chl-*a*, Steady-State (SS) ^{234}Th fluxes and POC fluxes at 100 m and euphotic zone (Ez) water depths for mid- vs. high salinity water and mid- vs. low salinity water.

Item	*P* value (Mid vs. High)	*P* value (Mid vs. Low)	Significance
POC, 0–100 m	0.0021	0.020	yes
Particulate Th, 0–100 m	0.000014	0.030	yes
Chl-*a*, 0–100 m	0.00031	0.00053	yes
Chl-*a*, 0-Ez bottom	0.0054	0.0018	yes
SS ^{234}Th flux@ 100 m	0.097	0.66	no
SS ^{234}Th flux@ Ez	0.051	0.79	no
POC flux@ 100 m	0.10	0.22	no

4.2 Comparison between low, mid- and high salinity waters showing insignificant export production enhancement in the STF

As shown in the Results section, Chl-*a*, POC and particulate ^{234}Th data suggest enhanced biological particle production in the upper 100 m of mid-salinity waters, compared to low and high salinity waters within the STF. This trend continues to hold if we integrate these data from the sea surface to 100 m water depth (Table 2). For example, the average inventories of Chl-*a*, POC and particulate ^{234}Th activities of $80 \pm 0.30\,\mathrm{mg\,m^{-2}}$, $(3.9 \pm 0.056) \times 10^2\,\mathrm{mmol\,C\,m^{-2}}$, and $(7.5 \pm 0.060) \times 10^2\mathrm{Bq\ m^{-2}}$, respectively, in mid-salinity waters, were high, compared to $40 \pm 0.30\,\mathrm{mg\,m^{-2}}$, $(2.5 \pm 0.022) \times 10^2\,\mathrm{mmol\,C\,m^{-2}}$, and $(3.4 \pm 0.030) \times 10^2\ \mathrm{Bq\ m^{-2}}$ in high salinity waters and $37 \pm 0.23\,\mathrm{mg\,m^{-2}}$, $(2.6 \pm 0.073)\ \times 10^2\,\mathrm{mmol\,C\,m^{-2}}$, and $(5.7 \pm 0.084) \times 10^2\,\mathrm{Bq\,m^{-2}}$ in low salinity waters. *T*-tests with unequal variance were carried out to compare the differences between the mid- and high salinity waters, and showed that *P* values ($\alpha = 0.05$) for Chl-*a*, POC and particulate ^{234}Th were 0.0031, 0.0021, and 0.000014, respectively (Table 3). *P* values would be 0.00053, 0.020, and 0.030, respectively for the same comparisons between mid- and low salinity waters. Such analyses indicate that the mid-salinity waters were statistically different from the other two water types. Note that the biological enhancement observed in the mid-salinity waters was also observed for primary production measured in a parallel study on the same cruise (Jill Schwarz, NIWA, personal communication). It is interesting that the enhancement of particulate ^{234}Th activity in mid-salinity waters was much stronger than for Chl-*a* and POC.

The high Chl-*a* biomass and/or PP levels in the STF have been well-defined in previous studies. For example, phytoplankton biomass in winter and spring were 4 and 6 times higher, respectively, in the STF than in adjacent low salinity SAW (Hall et al., 1999). The mean PP rate in winter could be as high as $22\,\mathrm{mmol\,C\,m^{-2}\,d^{-1}}$, which was 4 times higher than that in the SAW (Bradford-Grieve et al., 1999). Remote-sensing satellite data also show that the STF is characterized by year-round heightened pigment concentrations (Comiso et al., 1993; Murphy et al., 2001).

As described above, both DIN and PO_4 were replete. In comparison, $Si(OH)_4$ concentrations were in the range 0.39–3.4 $\mu\mathrm{mol\,l^{-1}}$, which might indicate inhibition of diatom growth according to Chang and Gall (1998). Nevertheless, we tend to believe that $Si(OH)_4$ was not yet limiting the PP because PP was significantly high at mid-salinity as compared to high salinity water regime despite the $Si(OH)_4$ concentrations being similar at these sites.

Moreover, other studies have proposed that the elevated iron levels caused by mixing induced by the shallow bathymetry of Chatham Rise and/or the atmospheric deposition from Australian dust may lead to such high biomass/PP levels in the STF to the east of New Zealand, a process frequently termed "natural iron fertilization". Indeed, Boyd et al. (2004) determined the dissolved iron concentrations and potential iron sources in a transect across the STF. Dissolved iron concentrations in frontal surface waters reached the highest values of $0.8\,\mathrm{nmol\,l^{-1}}$ (above the stress level of $0.2\,\mathrm{nmol\,l^{-1}}$) at about 43° S, which is coincident geographically with the crest of the Chatham Rise. Boyd et al. (2004) further noted that iron concentrations dropped dramatically to less than $0.2\,\mathrm{nmol\,l^{-1}}$ within 1 degree of latitude to the north of this location.

In contrast to the enhancement of PP within the STF, little difference in POC and ^{234}Th fluxes were found among the three water types identified in the present study. A *t*-test comparing the POC and ^{234}Th fluxes at the 100m export horizon between high and mid-salinity waters resulted in *P* values ($\alpha = 0.05$) of 0.097 and 0.10, respectively (Table 3). The same parameters were compared between the mid- and low salinity waters, and similar observations were apparent (see Table 3). These relationships still held when all parameters were integrated to the bottom of the Ez (instead of to a fixed norminal depth such as 100 m), which is not surprising given the fact that sinking particles originate mainly within the Ez and shallow re-mineralization has frequently been found just below this depth (e.g. Buesseler and Boyd, 2009). Thus, there was no difference in POC and ^{234}Th fluxes at 100 m and/or the base of the Ez between the three water types.

The reasons why the elevated PP levels in the STF frontal zone, especially in our mid-salinity waters, did not lead to an increase in POC export are still unclear. Note that our study area is characterized by abundant diatom production in most seasons (Boyd et al., 1999; Bradford-Grieve et al., 1997), which should have driven high POC export fluxes as in many oceanic regimes (Michaels and Silver, 1988). Therefore we suggest that there are other factors limiting POC export here. Similar scenarios of this decoupling between PP and POC export were also observed in most of the artificial iron fertilization experiments (see reviews by Boyd et al., 2007), and the limited export response was attributed to the consequence of complex functioning of the planktonic community structure (Buesseler et al., 2004) and/or bacterial re-mineralization and grazing pressure (dominance of microzooplankton grazing over mesozooplankton) (Boyd and Newton, 1995). In the present study, the most plausible reason causing the little enhancement of the export flux would be related to microzooplankton grazing. Indeed, Hall et al. (1999) demonstrated that >78 % of daily PP can be grazed by microzooplankton in the STF in austral spring and winter. In contrast, mesozooplankton grazing is likely to be in the order of only 1–2 % of daily PP (Bradford-Grieve et al., 1998). Unlike mesozooplanton, the fecal pellets produced

by microzooplankton are smaller and readily remineralized in the upper ocean and may not contribute significantly to export flux (Boyd and Newton, 1995; Michaels and Silver, 1988), as also suggested by other studies in the STF region (Nodder and Gall, 1998; Zeldis et al., 2002).

5 Conclusions

The present study applied a high resolution ^{234}Th sampling technique to define the magnitude and distribution of POC export in the STF region, which revealed with greater confidence that the POC export fluxes were on the order of 5.6 ± 0.81 to 30 ± 3.7 mmol C m^{-2} d^{-1}, with an overall average of 12 ± 0.41 mmol C m^{-2} d^{-1} ($n = 25$). There was little spatial variation among low, mid- and high salinity waters within the STF in austral autumn-winter, despite differences in biological particle production, as inferred from fluorescence/Chl-*a* profiles. The present study, on the other hand, confirmed that the STF region is characterized by elevated PP, in particular, in the mid-salinity waters ($34.5 < S < 34.8$), presumably stimulated by so-called natural iron fertilization processes (Boyd et al., 1999, 2004; Pollard et al., 2009).

The present study, therefore, implies that natural iron fertilization does not necessarily lead to the enhancement of POC export in STF regions. It must be pointed out that, compared to other natural/ artificial iron experiments (Boyd et al., 2007), the present study was carried out in a different season (late autumn-early winter cf. summer) and latitude (43-44° cf. >50–60°). Therefore, we anticipate that variations in temperature, latitude, season and oceanographic region will induce different ecosystem responses.

Acknowledgements. This study was funded by the Foundation of Science, Research and Technology (New Zealand) via the Coasts and Oceans Outcome-Based Investment (C01X0501). KZ was supported by a NIWA Capability Fund Visiting Scientist grant for him to participate in the cruise TAN0806. The preparation of the manuscript was supported by the National Natural Science Foundation of China through grant NSFC 40821063 to MHD. We thank the Captain, officers and crew of R/V Tangaroa for their assistance in sample collection during TAN0806, as well as other voyage participants, especially Steve George for operating the CTD. Thanks were also given to Karl Safi for supporting the macronutrient data. We finally thank Pinghe Cai and Ken Buesseler for their constructive comments on early drafts of this paper.

Edited by: C. Robinson

References

Bacon, M. P., Cochran, J. K., Hirschberg, D., Hammar, T. R., and Fleer, A. P.: Export flux of carbon at the equator during the EqPac time-series cruises estimated from ^{234}Th measurements, Deep Sea Res. II, 43, 1133–1153, 1996.

Behrenfeld, M. J. and Falkowski, P. G.: A consumer's guide to phytoplankton primary productivity models, Limnol. Oceanogr., 42, 1479–1491, 1997.

Benitez-Nelson, C. R., Buesseler, K. O., Karl, D. M., and Andrews, J.: A time-series study of particulate matter export in the North Pacific Subtropical Gyre based on ^{234}Th:^{238}U disequilibrium, Deep Sea Res. I, 48, 2595–2611, 2001a.

Benitez-Nelson, C. R., Buesseler, K. O., Rutgers van der Loeff, M.M., Andrews, J., Ball, L., Crossin, G., and Charette, M. A.: Testing a new small-volume technique for determining ^{234}Th in seawater, J. Radioanal. Nucl. Chem., 248, 795–799, 2001b.

Boyd, P. and Newton, P.: Evidence of the potential influence of planktonic community structure on the interannual variablity of particulate organic carbon flux, Deep Sea Res. I, 42, 619–639, 1995.

Boyd, P., LaRoche, J., Gall, M., Frew, R., and McKay, R. M. L.: Role of iron, light, and silicate in controlling algal biomass in subantarctic waters SE of New Zealand, J. Geophys. Res., Oceans, 104, 13395–13408, 1999.

Boyd, P., McTainsh, G., Sherlock, V., Richardson, K., Nichol, S., Ellwood, S., and Frew, R.: Episodic enhancement of phytoplankton stocks in New Zealand subantarctic waters: Contribution of atmospheric and oceanic iron supply, Global Biogeochem. Cy., 18, GB1029, doi:1029/2002GB002020, 2004.

Boyd, P., Jickells, T. D., Law, C. S., Blain, S., Boyle, E. A., Buesseler, K. O., Coale, K. H., Cullen, J. J., de Baar, H. J. W., Follows, M., Harvey, M., Lancelot, C., Levasseur, M., Owens, N. P. J., Pollard, R., Rivkin, R. B., Sarmiento, J., Schoemann, V., Smetacek, V., Takeda, S., Tsuda, A., Turner, S., and Watson, A. J.: Mesoscale Iron Enrichment Experiments 1993–2005: Synthesis and Future Directions, Science, 315, 612–617, 2007.

Bradford-Grieve, J. M., Chang, F. H., Gall, M., Pickmere, S., and Richards, F.: Size-fractionated phytoplanton standing stocks and primary production during austral winter and spring 1993 in Subtropical Convergence region near New Zealand., N. Z. J. Mar. Freshwater Res., 31, 201–224, 1997.

Bradford-Grieve, J., Murdoch, R. C., James, M., Oliver, M., and McLeod, J.: Mesozooplankton biomass, composition, and potential grazing pressure on phytoplankton during austral winter and spring 1993 in the Subtropical Convergence region near New Zealand, Deep Sea Res. I, 45, 1709–1737, 1998.

Bradford-Grieve, J. M., Boyd, P. W., Chang, F. H., Chiswell, S., Hadfield, M., Hall, J. A., James, M. R., Nodder, S. D., and Shushkina, E. A.: Pelagic ecosystem structure and functioning in the Subtropical Front region east of New Zealand in austral winter and spring 1993, J. Plankton Res., 21, 405–428, 1999.

Buesseler, K. O., Bacon, M. P., Cochran, J. K., and Livingston, H. D.: Carbon and nitrogen export during the JGOFS North Atlantic bloom experiment estimated from ^{234}Th:^{238}U disequilibria, Deep Sea Res., 39, 1115–1137, 1992.

Buesseler, K. O, Ball, L., Andrews, J., Benitez-Nelson, C. R., Belastock, R., Chai, F., and Chao, Y.: Upper ocean export of particulate organic carbon in the Arabian Sea derived from thorium-234, Deep Sea Res. II, 45, 2461–2487, 1998.

Buesseler K. O., Ball, L., Andrews, J., Cochran, J. K., Hirschberg, D. J., Bacon, M. P., Fleer, A. P., and Brzezinski, M. A.: Upper ocean export of particulate organic carbon and biogenic silica in the Southern Ocean along 170° W, Deep Sea Res. II, 48, 4275–4297, 2001a.

Buesseler K. O., Benitez-Nelson, C. R., Rutgers van der Loeff, M.M., Andrews, J., Ball, L., Crossin, G., and Charette, M. A.: An intercomparison of small- and large-volume techniques for thorium-234 in seawater, Mar. Chem., 74, 15–28, 2001b.

Buesseler, K. O., Andrews, J. E., Pike, S., and Charette, M. A.: The effect of iron fertilization on carbon sequestration in the Southern ocean, Science, 304, 414–417, 2004.

Buesseler, K. O., Benitez-Nelson, C. R., Moran, S. B., Burd, A., Charette, M., Cochran, J. K., Coppola, L., Fisher, N. S., Fowler, S. W., Gardner, W. D., Guo, L. D., Gustafsson, Ö., Lamborg, C., Masque, P., Miquel, J. C., Passow, U., Santschi, P. H., Savoye, N., Stewart, G., and Trull, T.: An assessment of particulate organic carbon to thorium-234 ratios in the ocean and their impact on the application of ^{234}Th as a POC flux proxy, Mar. Chem., 100, 213–233, 2006.

Buesseler, K. O., Lamborg, C., Cai, P., Escoube, R., Johnson, R., Pike, S., Masque, P., McGillicuddy, D., and Verdeny, E.: Particle fluxes associated with mesoscale eddies in the Sargasso Sea, Deep Sea Res. II, 55, 1426–1444, 2008.

Buesseler, K. O. and Boyd, P. W.: Shedding light on processes that control particle export and flux attenuation in the twilight zone of the open ocean, Limnol. Oceanogr., 54, 1210–1232, 2009.

Buesseler, K. O., Pike, S., Maiti, K., Lamborg, C. H., Siegel, D. A., and Trull, T. W.: Thorium-234 as a tracer of spatial, temporal and vertical variability in particle flux in the North Pacific, Deep Sea Res. I, 56, 1143–1167, 2009.

Cai, P. H., Dai, M. H., Lv, D. W., and Chen, W. F.: An improvement in the small-volume technique for determining thorium-234 in seawater, Mar. Chem., 100, 282–288, 2006.

Cai, P. H., Chen, W. F., Dai, M. H., Wan, Z. W., Wang, D. X., Li, Q., Tang, T. T., and Lv, D. W.: A high-resolution study of particle export in the southern South China Sea based on ^{234}Th: ^{238}U disequilibrium, J. Geophys. Res. Oceans, 113, C04019, doi:10.1029/2007JC004268, 2008.

Chang, F. H. and Gall, M.: Phytoplankton assemblages and photosynthetic pigments during winter and spring in the Subtropical Convergence region near New Zealand, N. Z. J. Mar. Freshwater Res., 32, 515–530, 1998.

Chen, J. H., Edwards, R. L., and Wasserburg, G. J.: ^{238}U, ^{234}U and ^{232}Th in Seawater, Earth. Planet. Sci. Lett., 80, 241–251, 1986.

Chen, W. F.: On the Export Fluxes, Seasonality and Controls of Particulate Organic Carbon in the Northern South China Sea, PhD dissertation, Xiamen Univ. Xiamen, China, 2008 (in Chinese).

Chiswell, S. M.: Variability in sea surface temperature around New Zealand from AVHRR images, N. Z. J. Mar. Freshwater Res., 28, 179–192, 1994.

Chiswell, S. M.: Variability in the Southland Current, New Zealand, N. Z. J. Mar. Freshwater Res., 30, 1–17, 1996.

Clementson, L. A., Parslow, J. S., Griffiths, F. B., Lyne, V. D., Mackey, D. J., Harris, G. P., McKenzie, D. C., Bonham, P. I., Rathbone, C. A., and Rintoul, S.: Controls on phytoplankton production in the Australasian sector of the subtropical convergence, Deep Sea Res. I, 45, 1627–1661, 1998.

Coale, K. H. and Bruland, K. W.: ^{234}Th:^{238}U disequilibria within the California Current, Limnol. Oceanogr. 30, 22–33, 1985.

Coale, K. H. and Bruland, K. W.: Oceanic stratified Euphotic Zone as elucidated by ^{234}Th:^{238}U disequilibria, Limnol. Oceanogr. 32, 189–200, 1987.

Cochran, J. K. and Masque, P.: Short-lived U/Th Series radionuclides in the ocean: tracers for scavenging rates, export fluxes and particle dynamics, Rev. Mineral. Geochem., 52, 461–492, 2003.

Comiso, J. C., Mcclain, C. R., Sullivan, C. W., Ryan, J. P., and Leonard, C. L.: Coastal Zone Color Scanner Pigment Concentrations in the Southern Ocean and Relationships to Geophysical Surface-Features, J. Geophys. Res. Oceans, 98, 2419–2451, 1993.

Coppola, L., Roy-Barman, M., Mulsow, S., Povinec, P., and Jeandel, C.: Low particulate organic carbon export in the frontal zone of the Southern Ocean (Indian sector) revealed by ^{234}Th, Deep Sea Res. I, 52, 51–68, 2005.

Dai, M. H. and Benitez-Nelson, C. R.: Colloidal organic carbon and ^{234}Th in the Gulf of Maine, Mar. Chem., 74, 181–196, 2001.

Froneman, P. W., McQuaid, C. D., and Laubscher, R. K.: Size-fractionated primary production studies in the vicinity of the Subtropical Front and an adjacent warm-core eddy south of Africa in austral winter, J. Plankton Res., 21, 2019–2035, 1999.

Gall, M., Hawes, I., and Boyd, P.: Predicting rates of primary production in the vicinity of the Subtropical Convergence east of New Zealand, N. Z. J. Mar. Freshwater Res., 33, 443–455, 1999.

Hall, J. A., James, M. R., and Bradford-Grieve, J. M.: Structure and dynamics of the pelagic microbial food web of the Subtropical Convergence region east of New Zealand, Aquat. Microb. Ecol., 20, 95–105, 1999.

Heath, R. A.: Oceanic Fronts around Southern New Zealand, Deep Sea Res., 28A, 547–560, 1981.

Heath, R. A.: A review of the physical oceanography of the seas around New Zealand–1982, N. Z. J. Mar. Freshwater Res., 19, 79–124, 1985.

Kara, A. B., Rochford, P. A., and Hurlburt, H. E.: An optimal definition for ocean mixed layer depth, J. Geophys. Res. Oceans, 105, 16803–16821, 2000.

Kawakami, H. and Honda, M. C.: Time-series observation of POC fluxes estimated from ^{234}Th in the northwestern North Pacific, Deep Sea Res. I, 54, 1070–1090, 2007.

Knap, A., Michaels, A., Close A., Ducklow, H., and Dickson, A.: Protocols for the Joint Global Ocean Flux Study (JGOFS) core measurements, JGOFS Report Nr. 19: vi-170 pp. (Reprint of the IOC Manuals and Guides No. 29, UNESCO 1994), 1996.

Longhurst, A.: Ecological Geography of the Sea, Academic Press, San Diego, Californiam 398 pp., 1998.

Michaels, A. F. and Silver, M. W.: Primary production, sinking fluxes and the microbial food web, Deep Sea Res., 35, 473–490, 1988.

Murphy, R. J., Pinkerton, M. H., Richardson, K. M., Bradford-Grieve, J. M., and Boyd, P. W.: Phytoplankton distributions around New Zealand derived from SeaWiFS remotely-sensed ocean colour data, N. Z. J. Mar. Freshwater Res., 35, 343–362, 2001.

Nodder, S. D.: Short-term sediment trap fluxes from Chatham Rise, southwest Pacific Ocean, Limnol. Oceanogr., 42, 777–783, 1997.

Nodder, S. D. and Alexander, B. L.: Sources of variability in geographical and seasonal differences in particle fluxes from short-term sediment trap deployments, east of New Zealand, Deep Sea Res. I, 45, 1739–1764, 1998a.

Nodder, S. D. and Gall, M.: Pigment fluxes from the Subtropical Convergence region, east of New Zealand: relationship to planktonic community structure, N. Z. J. Mar. Freshwater Res., 32,

441–465, 1998b.

Nodder, S. D. and Northcote, L. C.: Episodic particulate fluxes at southern temperate mid-latitudes (42–45° S) in the Subtropical Front region, east of New Zealand, Deep Sea Res. I, 48, 833–864, 2001.

Nodder, S. D., Pilditch, C. A., Probert, P. K., and Hall, J.: Variability in benthic biomass and activity beneath the Subtropical Front, Chatham Rise, SW Pacific Ocean, Deep Sea Res. I, 50, 959–985, 2003.

Nodder, S. D., Duineveld, G. C. A., Pilditch, C. A., Sutton, P., Probert, P. K., Lavaleye, M. S., Withbaard, R., Chang, F. H., Hall, J., and Richardson, K.: Focusing of phytodetritus deposition beneath a deep-ocean front, Chatham Rise, New Zealand, Limnol. Oceanogr., 52, 299–314, 2007.

Orsi, A. H., Whitworth III, T., and Nowlin Jr., W. D.: On the meridional extent and fronts of the Antarctic Circumpolar Current, Deep Sea Res. I, 42, 641–673, 1995.

Pollard, R. T., Salter, I., Sanders, R. J., Lucas, M. I., Moore, C. M., Mills, R. A., Statham, P. J., Allen, J. T., Baker, A. R., Bakker, D. C. E., Charette, M. A., Fielding, S., Fones, G. R., French, M., Hickman, A. E., Holland, R. J., Hughes, J. A., Jickells, T. D., Lampitt, R. S., Morris, P. J., Nédélec, F. H., Nielsdóttir, M., Planquette, H., Popova, E. E., Poulton, A. J., Read, J. F., Seeyave, S., Smith, T., Stinchcombe, M., Taylor, S., Thomalla, S., Venables, H. J., Williamson, R., and Zubkov, M. V.: Southern Ocean deep-water carbon export enhanced by natural iron fertilization, Nature, 457, 577–581, 2009.

Probert, P. K. and McKnight, D. G.: Biomass of bathyal macrobenthos in the region of the Subtropical Covergence, Chatham Rise, New Zealand, Deep Sea Res. I, 40, 1003–1007, 1993.

Redfield, A. C., Ketchum, B. H., and Richards, F. A.: The influence of organisms on the composition of sea-water, in: The Sea, 2, edited by: Hill, M. N., Interscience Publishers, John Wiley & Sons, 26–77, 1963.

Rutgers van der Loeff, M. M., Friedrich, J., and Bathmann, U. V.: Carbon export during the Spring Bloom at the Antarctic Polar Front, determined with the natural tracer ^{234}Th, Deep Sea Res. II, 44, 457–478, 1997.

Rutgers van der Loeff, M. M., Buesseler, K. O., Bathmann, U. V., Hense, I., and Andrews, J.: Comparison of carbon and opal export rates between summer and spring bloom periods in the region of the Antarctic Polar Front, SE Atlantic., Deep Sea Res. II, 49, 3849–3869, 2002.

Savoye, N., Benitez-Nelson, C. R., Burd, A. B., Cochran, J. K., Charette, M., Buesseler, K. O., Jackson, G. A., Roy-Barman, M., Schmidt, S., and Elskens, M.: ^{234}Th sorption and export models in the water column: a review, Mar. Chem., 100, 234–249, 2006.

Sutton, P.: Detailed structure of the Subtropical Front over Chatham Rise, east of New Zealand, J. Geophys. Res., Oceans, 106, 31045–31056, 2001.

Uddstrom, M. J. and Oien, N. A.: On the use of high-resolution satellite data to describe the spatial and temporal variability of sea surface temperatures in the New Zealand region, J. Geophys. Res., 104, 20729–20751, 1999.

Waples, J. T., Benitez-Nelson, C. R., Savoye, N., Rutgers van der Loeff, M. M., Baskaran, M., and Gustafsson, Ö.: An introduction to the application and future use of ^{234}Th in aquatic systems, Mar. Chem., 100, 166–189, 2006.

Zeldis, J., James, M. R., Grieve, J., and Richards, L.: Omnivory by copepods in the New Zealand Subtropical Frontal Zone, J. Plankton Res., 24, 9–23, 2002.